January 2013

The Role Of Fibroblast Growth Factors In Cortical Regeneration After Perinatal Hypoxia: A Model For Neurological Recovery In Premature Children

Devon Marc Fagel
Yale School of Medicine, devonfagel@gmail.com

The Role of Fibroblast Growth Factors in Cortical Regeneration After Perinatal Hypoxia: A Model For Neurological Recovery In Premature Children

A Thesis Submitted to the

Yale University School of Medicine

in Partial Fulfillment of the Requirements for the

Degree of Doctor of Medicine

By

Devon Marc Fagel, J.D.

2013

Abstract

Chronic perinatal hypoxia causes a significant loss of total brain volume, brain weight and cortical neuron number. These measures are completely reversed following recovery in normoxic conditions. Yet, the cellular and molecular mechanisms underlying this plasticity are not well understood. Here, we show that hypoxia from postnatal days 3 (P3) to 10-11 causes a 30% decrease in cortical neurons and a 24% decrease in cortical volume. Excitatory neuron numbers were completely recovered one month after the insult, but the mice showed a residual deficit in GABAergic interneurons. In contrast, hypoxic mice carrying a disrupted fibroblast growth factor receptor-1 (Fgfr1) gene in $GFAP^+$ cells [Fgfr1 conditional knock-out (cKO)], showed a persistent loss of excitatory cortical neurons and an increased interneuron defect. Labeling proliferating progenitors at P17-18 revealed increased generation of cortical $NeuN^+$ and $Tbr1^+$ neurons in wild-type mice subjected to hypoxic insult, whereas Fgfr1 cKO failed to mount a cortical neurogenetic response. Hypoxic wild-type mice also demonstrated a twofold increase in cell proliferation in the subventricular zone (SVZ) at P17-18 and a threefold increase in neurogenesis in the olfactory bulb (OB) at P48-49, compared with normoxic mice. In contrast, Fgfr1 cKO mice had decreased SVZ cell proliferation and curtailed reactive neurogenesis in the OB. Thus, the activation of Fgfr1 in $GFAP^+$ cells is required for neuronal recovery after perinatal hypoxic injury. In contrast, there is incomplete recovery of inhibitory neurons following injury, which may account for persistent behavioral deficits in adult mice following early perinatal injury.

Acknowledgements

First and foremost, I must thank the most important person in my life, my wife, Michelle. Ten years ago, I sat her down in our living room and asked “what do you think about me becoming a doctor.” We had been though years of school with each other. She had her master’s, I had my law degree. We were well prepared to make a home and raise a family. Then, in the midst of just starting out, I sprang this crazy idea on her. No experience with science, medicine or even math for that matter, beyond high school (unless you count my freshman “Astro-biology” course). Just a feeling that at some point we’d look back at that moment and take comfort in the fact that we made the right decision (though I know it hasn’t always seemed that way). I presented Michelle with a rough plan for the rest of our life or at least the next few years. Most newlywed wives would have shot the idea down before it left my mouth. But not Michelle. She said “why not” (my recollection of the conversation is far more cavalier than it probably really was). That was April. Cut to July and we’re on the road, two dogs in tow, driving across the country. That was a decade ago. Since then, Michelle gave me two beautiful children, Lila ViVi and Atticus James and I gave her a lot of stress and anxiety. Well, as we close this chapter of our life together and a new one begins, I look back at that moment with deep gratitude that she made the right decision. Thank you Michelle, I love you.

Okay so I know the part my wife played, but there are several other critical people without whom, this thesis wouldn’t exist and I’d likely be in LA practicing law. First is Dr. Flora Vaccarino. Not long after getting Michelle’s blessing, by way of serendipity, I found myself in Flora’s office relating my experiences of working with developmentally challenged kids in the courts and my desire for scientific evidence that no matter how severe their neurological deficits, a stable and loving home could provide lifelong benefits. Lacking scientific training, she recognized a compelling passion to study brain plasticity and a shared belief in the resiliency of children. Under her tutelage, this project began with the desire to challenge the central dogma of neuroscience, which held that the postnatal brain is an immutable organ, incapable of repair. Throughout, she offered independence and whenever needed, wise guidance.

Soon after my research began, as luck would have it, I wondered down the hallway of the Child Study Center and found the person who more than anyone else in my adult life, defined the word, mentor, Dr. Andres Martin. He took the time to teach a pre-pre-med student that medicine was not solely a scientific endeavor but an art. Still years away from learning how to conduct an H&P, he ~~taught~~ demonstrated how patients respond to empathy, even when conventional treatments have failed them.

As I embark on the next step, I am grateful to call Flora and Andres, not just mentors, but friends. But still there are a few more people whom without, I wouldn’t be able to take that next step. Dr. Nancy Angoff; what can I say, if I could design the perfect Jewish Mother, it would be her. Through many, many office visits, she has provided just the right mix of love and support, discipline and authority, with just a hint of guilt for good measure. Finally, a special acknowledgment for the single person who got the whole ball rolling, Dr. James Leckman. My first time at Yale, he picks me up and shuttles me around the entire campus to meet a select group of researchers who he thought would give me a chance. At the end of a long day, he asked, “are you up to meeting just one more person” and walked me into Flora’s lab, where this thesis begins.

Table of Contents

Introduction

Very low birth weight (VLBW) preterm infants comprise 2% of all live births. This poses a substantial public health problem, both in the pediatric population and possibly later in life (Hack et al., 2002; Als et al., 2007). Despite improved survival rates approaching 85% for preterm infants weighing less than 1500g (Fanaroff et al., 2007), half of these children sustain cognitive and neurodevelopmental disabilities. However, recent long-term studies demonstrate progressive improvement over time in children without grade 3/4 intraventricular hemorrhages or significant white matter injury (Ment et al., 2003; for a review, see Saigal and Doyle, 2008), suggesting a capacity for recovery which has yet to be fully investigated. Despite early differences, serial neurocognitive evaluations have demonstrated progressive improvement such that by adolescence, language scores for preterm subjects approach those of term controls (see review by Saigal and Doyle, 2008; Ment et al., 2003). This long-term behavioral outcome is paralleled by significant structural plasticity in the preterm brain. For example, while there are decreases in brain volume at birth (Peterson et al., 2003; Inder et al., 2005a), there appear to be no significant difference in total volume measures as these children reach adulthood (Fearon et al., 2004; Allin et al., 2007). However, subtle differences in the volume of subcortical structures and ventricular enlargement persist (Allin et al., 2004; Fearon et al., 2004). A voxel-based morphometry study (Nosarti et al., 2008) found that there were not only regions of loss but interestingly other areas with relatively greater volumes when preterm adolescents were compared to term controls at 14–15 years of age. This increase in the volume of certain regions was more prominent in preterm children that had neonatal ultrasound evidence of periventricular hemorrhage

and ventricular dilation, suggesting that in cases of more severe brain injury, the brain appears to compensate by increasing cell number in order to adapt. Yet even in preterm infants without evidence of periventricular hemorrhage and ventricular dilation, the grey matter in the cingulate, temporal and parahippocampal gyri and white matter in the frontal, parietal and occipital cortices were increased. It is not clear whether these increases are a compensatory mechanism for injury or a delay in the natural maturation process resulting in the absence of age appropriate pruning. Further, the mechanisms responsible for these long-term alterations are not well understood.

Magnetic resonance imaging (MRI) has demonstrated not only structural but functional differences in the brain development of preterm children compared to term controls from infancy to early adolescence (Ment et al., 2009; Inder et al., 2005a; Gimenez et al., 2006a,b; Nosarti et al., 2008; Srinivasan et al., 2007). At all ages studied, preterm children have smaller volumes in certain brain regions including cerebral grey matter, basal ganglia and cerebellum (Inder et al., 2005a; Nosarti et al., 2008). Recent advances in imaging technology such as diffusion tensor imaging (DTI), allowing for the evaluation of microstructural alterations, have revealed changes in white matter organization and function. DTI provides quantitative measurements of fractional anisotropy (FA), or the degree to which water diffusion is restricted in one direction compared to others. MRI studies have confirmed that preterm children demonstrate FA differences at birth through adolescence (12–15 years of age) (Constable et al., 2008; Skranes et al., 2007).

Numerous factors, genetic as well as environmental have been hypothesized to influence cognitive development and micro-structural changes in the developing brain. Als et al. (2004) found that low-risk preterm infants enrolled in a Newborn Individual Developmental Care and Assessment Intervention Program (NID-CAP) had greater FA in the internal capsule and frontal region white matter than those who did not receive this care, suggesting that activity-dependent mechanisms may have a significant impact on the degree of structural and functional recovery. These studies suggest that environmental and perinatal events may influence brain development. Genetics may also play a role. It is well established that overall white matter fiber architecture is genetically pre-programmed, with the understanding that the cortical milieu can alter their programmed trajectory. In a study of monozygotic and dizygotic twins using FA and DTI, white matter integrity was highly heritable and correlated with their performance on intelligence quotient measures (Chiang et al., 2009). It has also been shown that grey matter structures in frontal, sensorimotor and language related cortices are heritable in the monozygotic compared to dizygotic twins (Thompson et al., 2001).

It is difficult to disentangle the respective contribution of the degree of injury and environmental and genetic variables responsible for both the apparent gross recovery of preterm infants as well as the more subtle, long-term differences. Additionally, it is likely that these factors interact with each other to condition the variable response to injury. In order to better understand the environmental and genetic factors contributing to the outcome of preterm children, these variables must be studied independently and in their reciprocal interactions with each other. Given obvious reasons, human studies and interventions are fairly limited. Therefore the study of premature brain injury is based in

large part on animal models. This also provides the opportunity to study genetically altered mice, to knock-out or over-express individual genes of interest. Yet for an animal model to be relevant it must accurately reflect the histopathological spectrum of a specific injury to the developing brain, correlate with developmental changes observed in children and display the functional outcomes seen in human pathology. Various investigators have studied neonatal brain injury using different methods to induce injury, resulting in neuropathological changes that resemble those found in humans. In order to mimic the injury and outcome of less severely affected preterm children, we have focused on a model of perinatal hypoxia among a wild-type mouse population as well as those that have been genetically modified.

The premature infant is subject to failure in oxygenation due to immature lungs and respiratory disturbances resulting in hypoxia. This is an important contributor to brain injury in premature infants and results in altered neuronal differentiation and synaptogenesis as well as a loss of neurons, glia and their progenitors due to increased apoptosis. There are two main models of hypoxia, which are not mutually exclusive, chronic and intermittent (Fagel et al., 2006; Douglas et al., 2007). We have chosen to focus all of our studies on a model of chronic perinatal in which mice are subjected to sublethal hypoxia during the first 10-11 days after birth, a period of rapid brain development, resulting in very consistent results, namely global injury and long-term behavioral impairment. First, we exposed mice pups to hypoxia (9.5–10.5% O2) from P3 to P11 followed by recovery in normoxic conditions until P49. These mice initially suffer ventriculomegaly and a significant loss of cortical neuron number, cortical volume and brain weight as well as a diminished corpus callosum and subcortical white matter

(Fagel et al., 2006). Similar to findings in human studies on preterm infants, the initial decrease in cortical grey matter, subsequently makes a full recovery. However, mice subjected to hypoxia suffer long-term neurobehavioral sequelae including hyperactivity, increased anxiety (Weiss et al., 2004) and impairment in learning tasks and discrimination (Dell'Anna et al., 1991; Nyakas et al., 1996). While the hyperactivity subsides within several weeks, working memory and other impairments appear to be permanent (Chahboune et al., 2009). Taken together, our data suggest that this model causes alterations in brain development similar to those found in humans.

The early postnatal brain has a unique capacity to recover from various types of developmental injuries. This plasticity can be attributed to the reorganization of existing circuitry, via neurogenesis, synaptogenesis and differential axon growth and guidance. Studies utilizing various injury models have shown that the postnatal brain contains an endogenous pool of multipotent progenitor cells with the ability to proliferate and differentiate into new neurons and glial cells following insult (Fagel et al., 2006, 2009; Plane et al., 2004; Felling et al., 2006; Yang et al., 2007). The germinative zones where these cells reside are the subgranular layer of the hippocampal dentate gyrus and the subventricular zone (SVZ) adjacent to the lateral ventricles of the forebrain. Precursor cells may also exist in the latent stage in white matter and diffusely in grey matter (Palmer et al., 1999). The SVZ has been of particular interest in our studies because in humans it plays a prominent role during mid to late gestation (corresponding to the first perinatal week in mice). Other studies have demonstrated that during this critical period, the SVZ is comprised of immature cell types that are at different stages of lineage restriction with the capacity to provide neural precursors in the event of perinatal injury

(Yang and Levison, 2006). In both humans and mice, slowly dividing GFAP+ multipotent progenitor cells in the hippocampus and the SVZ neurogenic niches give rise to proliferating neural progenitors which in turn produce new neurons, thus enabling recovery (Doetsch et al., 1999). While progenitor cells proliferate as a normal response, premature birth likely alters the natural course of development for these cells.

Our studies focused primarily on neuronal cell populations and examined the long-term developmental and morphological outcomes. Mice subjected to chronic perinatal hypoxia from P3 to P10-11 suffered a 30% decrease in brain weight, cortical volume and neuron specific neuronal nuclei (NeuN)+ neuron number in the cerebral cortex immediately after cessation of injury. However, after one week of recovery in normoxic conditions, the hypoxic reared mice showed a substantial increase in the number of proliferating cells, marked by the incorporation of 5-bromo-2-deoxyuridine (BrdU), many of which co-expressed astroglial markers, including vimentin, brain lipid binding protein (BLBP) and astrocyte-specific glutamate transporter (Fagel et al., 2006). Cells of the radial glial lineage express these proteins during embryogenesis, giving rise to neural precursors (Feng et al., 1994; Shibata et al., 1997). To examine the fate of the proliferative precursors, BrdU was incorporated into these cells one week after the cessation of hypoxia and a detailed analyses of the long-term fate of BrdU+ cells was performed. Our study revealed a two-fold increase in the number of BrdU+ cells in the cortex four weeks after the insult, and a parallel increase in neurogenesis as well as gliogenesis, with no changes in the proportion of differentiated neurons, astrocytes and oligodendrocytes (Fagel et al., 2006). Our more recent studies examining the genesis of different neuronal subtypes revealed a preferential generation of T-brain-1 (Tbr1)+

excitatory as opposed to Parvalbumin+ and Calretenin+ inhibitory neurons (Fagel et al., 2009). This mismatch may correlate with the long-term cognitive deficits that these hypoxic mice continue to exhibit and may provide a clue for future interventions.

The nature of injury may also play a determinant role in recovery. For example, adult rodents that suffer infarct-producing ischemic events can regenerate striatal and hippocampal neurons, but not cortical neurons (Yoshimura et al., 2001; Arvidsson et al., 2002; Parent et al., 2002; Hoehn et al., 2005), whereas diffuse neuronal apoptosis stimulates the genesis of cortical projection neurons from endogenous progenitors (Magavi and Macklis, 2002). Others have reported the generation of cortical inhibitory interneurons after perinatal hypoxia-ischemia, although many of these cells appear to be transient (Yang et al., 2007). Prior to our work, neurogenesis had yet to be seen in adult rodent or macaque cerebral cortex, under basal conditions (Kornack and Rakic, 2001). In the mammalian CNS, neurogenesis is thought to be limited to the embryonic period; the only exceptions being the olfactory bulb (OB) and hippocampal dentate gyrus (DG), in which neurogenesis continues throughout life (Altman and Das, 1965; Gage, 1998; Lois and Alvarez-Buylla, 1993; Luskin, 1993). Despite the paucity of evidence of postnatal cortical neurogenesis, we set out to test our hypothesis that neurogenesis can occur constitutively in the immature cortex and that it plays a role in recovering neurons after hypoxic damage. Still, the mechanism remained illusive.

In order to understand the neurobiological substrates responsible for premature brain injury, altered developmental trajectories, and the potential for recovery, molecular manipulation of key regulatory proteins and genes are necessary. This is difficult in large

animal models, thus necessitating investigation using mice. Advances in murine genetics and in the understanding of the molecular mechanisms that regulate gene expression have allowed scientists to develop null-mutant or transgenic mouse strains to examine the role of specific genes in the response to injury. For example, it is known that during embryogenesis, key secreted factors play a critical role in brain development such as fibroblast growth factor (FGF), insulin like growth factor (IGF), vascular endothelial growth factor (VEGF), epidermal growth factor (EGF), brain-derived neurotrophic factor (BDNF), and Sonic Hedgehog (SHH). In the postnatal brain, these factors continue to be expressed in the SVZ. Many of these factors show altered expression after injury. We hypothesized that FGF may play the most important role in recovery and thus we focused our studies on this growth factor.

Neurogenesis in the embryonic and perinatal periods is regulated by FGF (Tao et al., 1996; Vaccarino et al., 1999a, 2001). FGF can induce neural fate in uncommitted stem cells (Stavridis et al., 2007) and increase progenitor proliferation (Vaccarino et al., 1999b; Wagner et al., 1999). In the embryonic cortex, Fgf2 increases the number of neural progenitors (Raballo et al., 2000) and the differentiation of inhibitory as well as excitatory neurons (Dono et al., 1998; Ortega et al., 1998; Vaccarino et al., 1999b; Shin et al., 2004). Further, both endogenous Fgf2 (Yoshimura et al., 2001) and exogenously administered Fgf2 (Nakatomi et al., 2002; Androutsellis-Theotokis et al., 2006; Monfils et al., 2006) promote neurogenesis in the DG and behavioral recovery after a number of injuries in adult rodents, including mechanical motor cortex injury, local cortical ischemic lesions and global hypoxia-ischemia.

Indeed, our initial studies demonstrated that FGF gene expression is upregulated in various brain regions following hypoxia, possibly leading to the appearance of radial glial type cells, a subset of which co-express FGF receptor 1 (Fgfr1) (Ganat et al., 2002). This led to speculation that astroglial cells respond to perinatal injury either by reverting back to immature radial glia or that injury during this critical period hinders normal maturation of radial glial into GFAP+ astrocytes, diverting their differentiation away from glial and towards neuronal progenitor cells. Using mice with a disrupted Fgfr1 gene in GFAP+ cells, we assessed whether this FGF receptor may be responsible for reconstituting brain structure after chronic sublethal hypoxic injury and the role of neurogenesis in this process. An unbiased stereological analysis of the number of newly generated cortical and olfactory bulb neurons was performed in parallel with an assessment of the total number of excitatory and inhibitory neurons several weeks after the insult. The data suggest that Fgfr1 signaling is required not only for cell proliferation and neurogenesis after an insult, but also for indirect effects leading to enhanced neuronal survival or maturation in the post-hypoxic environment.

Methods

Mouse Lines

Initial studies were conducted on wild-type C57/Bl mice. Later experiments utilized a knockout mouse model to study the role of a specific gene. To conditionally knockout the Fgfr1 gene, mice carrying the $Fgfr1^{f}$ allele (Trokovic et al., 2003) were crossed with $GFAP^{Cre}$ mice, which express Cre under the control of the human GFAP promoter (Zhuo et al., 2001). The $Fgfr1^{f/f;hGFAP\ Cre}$ mice lack Fgfr1 gene expression in telencephalic precursors, as described previously (Ohkubo et al., 2004; Smith et al., 2006). Cre negative littermate mice were used as controls. The genetic background of the knockout mice is a mixed 129/Sv, C57/BL, FVB and CD1. All experimental procedures were performed in accordance with the Yale Animal Resources Center and Institutional Animal Care and Use Committee policies.

Hypoxic Rearing

The experimental paradigm is schematized in Fig 1. C57/Bl mice were placed in an airtight Plexiglas hypoxia chamber maintaining a 9.5 – 10.5% O2 concentration by displacement with N2 as described previously (Ganat et al., 2002; Turner et al., 2003; Weiss et al., 2004). Hypoxia was begun at postnatal day 3 (P3) and was continued for 24 h in one group (P4) or for 8 days (P11) in all other mice. A separate group of control, normoxic mice were used and matched for strain, age, and supplier. Due to a diminished survival rate among the cKO mice, this group (as well as its normoxic counterparts) received one less day of hypoxia ending at P10 instead of P11. Both hypoxic-reared and normoxic mice (four to eight mice per group) were fostered to CD1

dams. In Fig 1, the hypoxia period is represented by a shaded bar on the thick black line. Mice were analyzed at various times after hypoxia (represented by marks on the thick black line in Fig. 1) with previous injection(s) of 5- bromo-3-deoxyuridine (BrdU) (see below). cKO mice were sacrificed at P10, P17 or P48. Mice were perfused transcardially with 20 ml of PBS followed by 35 ml of 4% paraformaldehyde (PFA). Brains were postfixed overnight in PFA, cryoprotected in a 20% sucrose solution overnight, and stored at -80°C after embedding in Tissue-Tek O.C.T. Compound (Electron Microscopy Sciences) medium.

2-Bromodeoxyuridine Birthdating Assay

BrdU (4 mg/ml in 0.007 N HCl/0.9% NaCl, Sigma) was administered intraperitoneally (50 mg/kg) every 4 hours at either P18 or P17 (0, 4, 8 and 12h), and animals were killed at 14h or 31d later. In both cases, the total labeling time was ~14 h, since BrdU avail- ability time is estimated to last for 4–5 h after injection (Hayes and Nowakowski, 2000). The reason for this cumulative labeling protocol is that it should label all constitutively proliferating cells of the subventricular zone (SVZ), as their cell cycle is ~13 h (Zheng et al., 2004). Based on double labeling of BrdU and 3H thymidine, this dosage of BrdU has been shown to label S-phase cells (Nowakowski et al., 1989; Hayes and Nowakowski, 2000).

Immunohistochemistry

In most cases, free-floating immunocytochemistry in serial sections was used. Brains were serially sectioned at 50 um thickness, and sections were stored in 0.04% sodium azide (NaN3)/PBS solution at +4°C. For BrdU immunostaining, sections were

washed in PBS, incubated in 1.5 N HCl at 37-C for 30 min, washed 3 times with PBS, blocked in 0.1% Tween-20/0.2% Triton in PBS (PBS++) containing 10% normal goat serum (NGS/PBS++), and then incubated in either mouse anti-BrdU (1:500, Becton-Dickinson, San Jose, CA) or rat anti-BrdU (1:500, Accurate Chemical, Westbury, NY) overnight at 4-C in 5% NGS/PBS++. Sections were then washed 3 times with PBS and incubated for 1 h in anti-mouse Alexa 594 (1:500, Molecular Probes, Eugene, OR) or anti-rat rhodamine cross-absorbed (1:400, Jackson, West Grove, PA) in 5% NGS/PBS+, washed again, mounted, and coverslipped using Vectashield with DAPI (Vector, Burlingame, CA).

The following primary antibodies were used: mouse anti-NeuN (1:500, Millipore), rabbit anti-Tbr1 (1:1000) (gift from Dr. Hevner, University of Washington School of Medicine, Seattle, WA), mouse anti-SMI-32 (1:1000; Covance), rabbit anti-caspase-3 (1:500, Cell Signaling, Beverly, MA), rabbit anti-S100h (1:300, Sigma), rabbit anti-GLAST (astrocyte-specific glutamate transporter, 1:2000, kind gift from Dr. Watanabe, Hokkaido University, Sapporo, Japan), rabbit anti-BLBP (brain lipid-binding protein, 1:1000, kind gift from Dr. Heintz, Rockefeller University, New York, NY), mouse anti-GFAP (glial fibrillary acidic protein, 1:400, Sigma), mouse anti-Mash1 (1:10, kind gift from Dr. Guillemot, National Inst. of Medical Research, The Ridgeway Mill Hill, United Kingdom), rabbit anti-GFAP (1:500, Sigma), mouse anti-PSA-NCAM (polysialic acid-NCAM, 1:400, Chemicon), rabbit anti-DLX-2 (1;100, kind gift from Dr. Rubenstein, University of California at San Francisco, San Francisco, CA), mouse anti-Rip (1:500, Chemicon), mouse anti-HuC/HuD (1:500, Molecular Probes), mouse anti-GABA (g-aminobutyric acid, 1:500, Sigma), and goat anti-Dcx (doublecortin, 1:500, Santa Cruz,

Santa Cruz, CA), mouse anti-Parvalbumin (PV) (1:2500, Sigma), rabbit anti-Calretinin (CR) (1:2000, Millipore), rat anti-BrdU (1:500, Accurate Chemical), mouse anti-Fgfr1 (1:500, Upstate), rabbit anti-Sox2 (1:3000, Millipore), rabbit anti-Pax6 (1:1000, University of Iowa, Iowa City, IA) and rabbit anti-Tbr2 (1:2000, gift from Dr. Hevner). The following secondary reagents were also used: anti-mouse Alexa 488 (1:500, Molecular Probes, Invitrogen), anti-mouse Alexa 488 cross absorbed (1:500, Molecular Probes, Invitrogen), anti-rabbit Alexa 594 (1:700, Molecular Probes, Invitrogen), anti-rabbit Alexa 488 (1:1000, Molecular Probes, Invitrogen), anti-mouse rhodamine red cross absorbed (1:400, Jackson), anti-mouse, anti- goat, and anti-rabbit biotinylated (1:200, Vector), and avidin flourescein (1:1000, Vector). For immunoperoxidase detection, the ABC Elite kit (Vector) was used as directed.

For detection of migrating neuroblasts and evaluation of differentiated BrdU labeled cells, brains were perfused with 2% PFA in PBS, and 10 Am-thick cryostat sections were collected serially and stored at -80°C. Series of 1:50 sections were reacted directly on slides. The immunoflourescent procedure described above was followed except that sections were blocked in 0.1% Triton in PBS (PBS+) containing 10% NGS (NGS/PBS+) and incubated in a cocktail containing the primary antibodies in 10% NGS/PBS+ for 48 h at 4-C. For fluorescent labeling of Dcx-positive cells, sections were washed in 1% Triton in PBS for 15 min and then processed with secondary reagents as described above.

Morphometry and Cell Counting

Unbiased estimates for volumes and cell numbers were obtained using a computer coupled to a Zeiss Axioskope 2 Mot Plus, running the StereoInvestigator software with Neurolucida (Microbrightfield). For the cortex, one in every twenty serial sections were selected for analyses; for the SVZ and OB, one in every ten sections were selected. Contours were drawn around the cerebral cortex including the infralimbic, orbital, cingulate, entorhinal and retrosplenial cortices, and cell counting was performed as described previously (Korada et al., 2002; Fagel et al., 2006). To estimate the total number of newly generated neurons in the cortex, $NeuN^+/BrdU^+$ cells as well as $Tbr1^+/BrdU^+$ and $SMI\text{-}32^+/Tbr1^+$ cells were simultaneously visualized by a 594 and 488 nm double-exposure filter and counted using the optical fractionator method in a 3-dimensional counting frame of 100 x 100 x 5 um using a sampling grid of 1500 x 1500 um for NeuN, 750 x 750 um for Tbr1 and 1000 x 1000 um for SMI-32, PV and CR. At P10, 5–6 coronal sections were sampled per brain, whereas at P48, 6–7 sections were sampled. Approximately 40 NeuN, 180 Tbr1 and 120 SMI-32, PV and CR sampling sites were counted for each cortex. The contours of the granular layer of the OB were drawn based on its increased cellular density in DAPI-stained sections. To estimate the total number of $Neun^+/ BrdU^+$ cells in the OB, cells were counted in a counting frame of 50 x 50 x 5 um, using a sampling grid of 500 x 500 um. At P48, 5–6 coronal sections and ~50 sampling sites were counted for each OB. Cells were classified as double-stained only if both colors were in sharp focus within a narrow (~2 um) focal plane, using the z-axis encoder. The contours of the SVZ were drawn based on its increased cellular density in

DAPI-stained sections and included the entire extent of the SVZ from its rostral end until the beginning of the hippocampal commissure. To estimate the total number of $BrdU^+$ cells in the SVZ, cells were counted in a counting frame of 50 x 50 x 5 um, using a sampling grid of 200 x 200 um. Between 3 and 4 coronal sections and ~25 sampling sites were counted for each SVZ. The average Schaffer coefficient of error for cell counting was 0.04 – 0.07 for cortex, 0.06 – 0.10 for OB and 0.15– 0.17 for SVZ.

Statistical Analyses

The percent difference was defined as the mean of hypoxia minus the mean of normoxia divided by the mean of normoxia. P values were calculated from the t test and validated by nonparametric Wilcox test (the results are generally consistent between the two tests, and the P values from the Wilcox test are not reported). Data were also analyzed by ANOVA or Student's t test using the DataDesk statistical program. The number of samples is specified in each case in the figure legends. Post hoc analyses were performed via the Sheffe post hoc test.

Results

Transient cell loss following chronic perinatal hypoxia

Mice were exposed to sublethal hypoxia for 8 days, from P3 to P11 (shaded bar in Fig. 1). Although 24 h of hypoxia was not sufficient to cause any apparent changes in brain weight, by P11, there was a statistically significant 24% decrease. This was fully reversed after 7 days of normoxia (Table 1). To confirm that the weight loss was due to structural brain abnormalities, we examined serial sections stained with cresyl violet. Consistent with previous findings using this model (Turner et al., 2003), we found an increase in ventricular volume as well as a thinning of the cerebral cortical mantle at P11 (Figs. 2A,B). To investigate whether these morphometric changes were due to a loss of neurons, we immunostained serial sections with NeuN, a marker for neuronal cell nuclei, and estimated cortical volume and neuron number by unbiased stereological techniques. Hypoxic-reared mice were found to have a 30% loss of neurons in the cerebral cortex at P11 and a corresponding decrease in cortical volume (Figs. 3E,F). To determine what types of neurons were vulnerable to hypoxia, we immunostained the P11 brain with SMI-32, a monoclonal antibody that recognizes a non-phosphorylated neurofilament epitope in pyramidal neurons of the cerebral cortex. Qualitative examination of SMI-32 immunostaining revealed decreased density of pyramidal cells within the P11 cortex (Figs. 2 C–F).

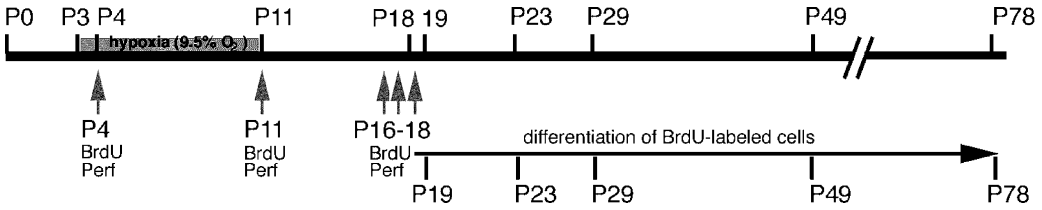

Figure 1. Timeline of the experiment. Shaded bar indicates chronic hypoxic exposure, and shaded arrows indicate injection of BrdU. Hypoxia was begun at P3 and continued for 24 h in one group (P4) or for 8 days in all other mice (P11). To assess proliferation, a single BrdU injection was administered at P4, P11, and P18, and mice were perfused after 30 min. To assess differentiation, the same dose was cumulatively delivered every 4 h beginning at P18 for a total labeling of 16 h or every 6 h beginning at P16 for a total of 54 h (multiple arrows between P16 and P18). BrdU-injected mice were allowed to survive for 1, 5, 11, 31, or 60 days (marks on black arrow corresponding to P19, P23, P29, P49, and P78).

Brain weights (mg)

	P4	P11	P18	P49	P78
Days of hypoxia/ recovery	1/0	8/0	8/7	8/31	8/60
Normoxic	170 ± 4.0	335 ± 13	381 ± 16.3	463 ± 9.1	462 ± 15.7
Hypoxic	173 ± 4.9	255 ± 6.6*	385 ± 3.6	431 ± 13.7	450 ± 26.5
% decrease	−1.8%	23.9%	−1%	6.9%	2.6%

Table 1. Mice were exposed to a PO2 of 9.5% beginning at P3 for 1 day (P4) or 8 days (P11) then allowed to recover in a normoxic environment for a variable period of time as indicated. N = 8 for all time points.
* $P < 0.01$, Student's t test.

The most remarkable aspect of this model was that one week after the cessation of injury, hypoxia-induced changes were apparently reversed in these mice. Thus at P18, hypoxic-reared mice were indistinguishable from normoxic mice with respect to brain weight (Table 1), cortical volume, and number of NeuN-positive cells in the cerebral cortex (Figs. 3E,F). Similarly, hypoxic-reared mice did not show substantial differences in the density of neuronal cell bodies immunostained with Parvalbumin (PV), Calbindin (CA), or SMI-32 at this age. SMI-32 staining in the neuropil of the cerebral cortex and the basal ganglia, however, remained decreased in mice recovering from hypoxia; and specifically, although in control tissue most pyramidal cells had already extended a prominent apical dendrite, such dendrites were still absent in hypoxic cortical tissue.

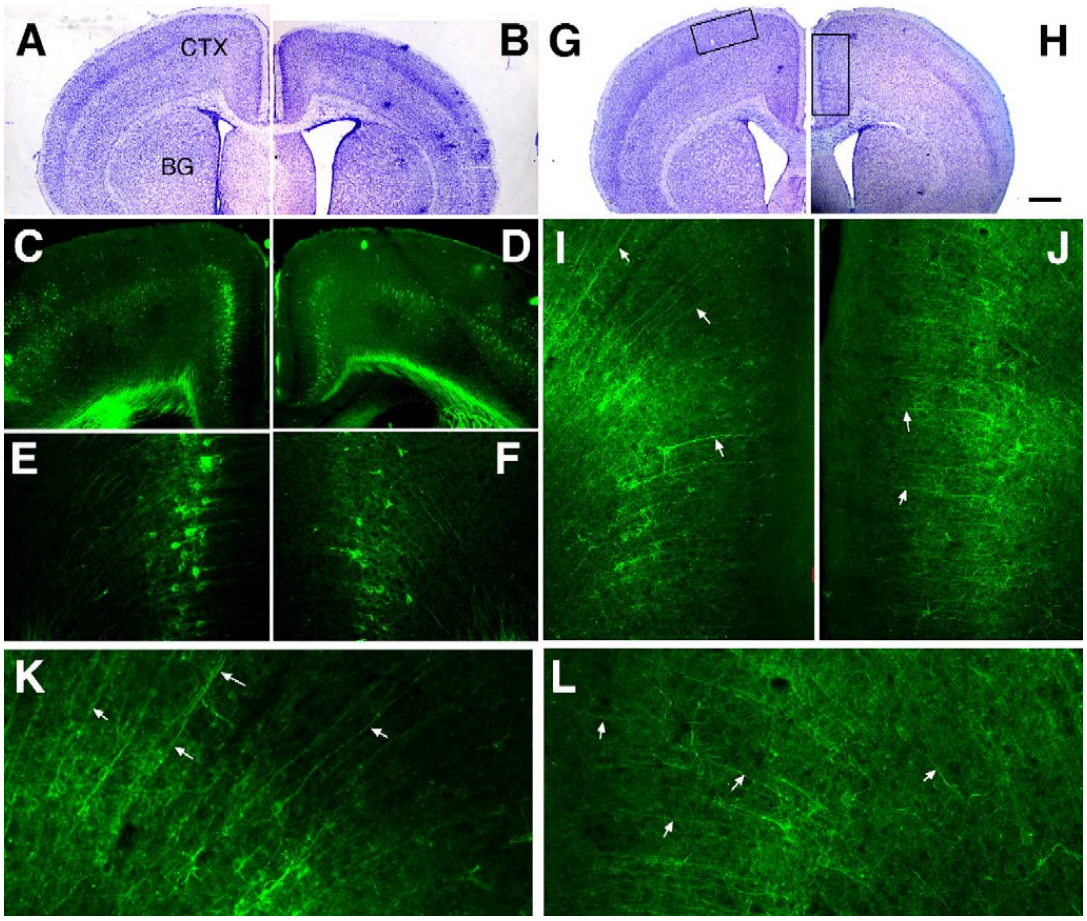

Figure 2. Volume and neuron number are decreased in hypoxic brains at P11 and recovered at P49. (A, C, E, G, I, K) Normoxic and (B, D, F, H, J, L) hypoxic brains (coronal sections). (A–B) Cresyl violet-stained sections at P11 showing decreased forebrain volume and ventriculomegaly after hypoxia. (C–F) SMI-32 immunostaining at P11; panels (E) and (F) are high power images of panels (C) and (D), respectively, showing decreased number of pyramidal neurons in the medial prefrontal cortex in hypoxic brains. (G–H) Cresyl violet staining at P49 showing recovered volume of the anterior cerebral cortex in hypoxia. (I–L) SMI-32 immunostaining at P49 showing normal neuronal density but decreased dendritic arborization in hypoxic mice in medial prefrontal (I, J) and dorsolateral prefrontal cortex (K, L). Scale bar = 200 Am in A, B; 100 Am in C, D and G, H; 25 Am in E, F and I–L.

To address the permanence of these effects, we examined hypoxic-reared mice at P49, after 31 additional days of recovery, as compared to normoxic controls. There was no significant difference among hypoxic and normoxic mice in volume or number of neurons for the cerebral cortex, the hippocampus and the basal ganglia (Figs. 2G,H; Figs. 3E,F; Table 2). The only detectable abnormality at P49 was a subtle change in pyramidal cell dendritic arbors in the cerebral cortex, which appeared much thinner and

less regularly arrayed as revealed by SMI-32 immunostaining (Fig. 2, arrows in I,K and J,L). Together, these data suggest that perinatal hypoxia causes an initial loss of cortical neurons that may be responsible in part for the decrease in brain weight and volume and the ventriculomegaly. These abnormalities were recovered over the ensuing period of normoxia, except for a persistent disorganization of cortical neuropil.

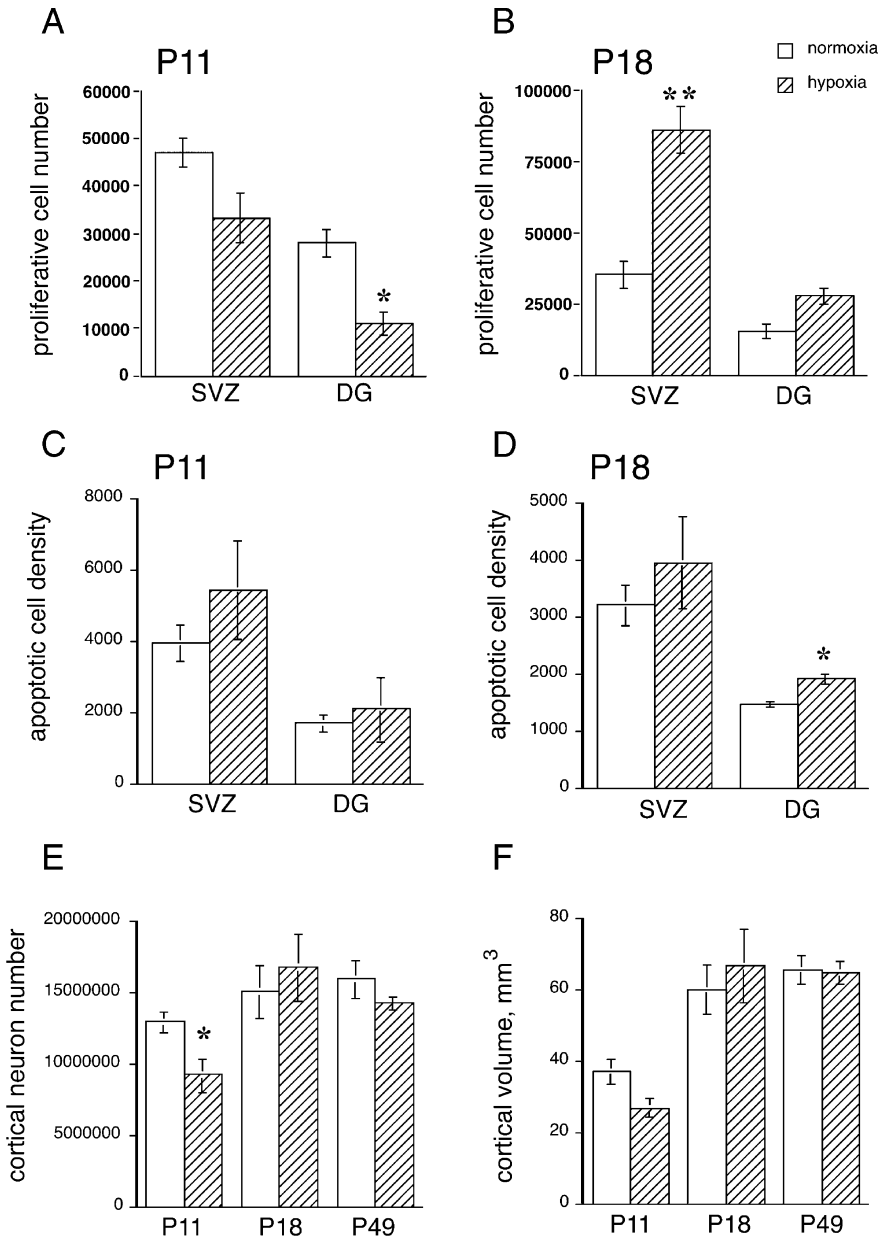

Figure 3. Number of proliferative cells, apoptotic cell density, and morphometric analysis of the cerebral cortex in hypoxic mice. (A) Number of BrdU-positive cells in the neurogenic areas of control (open bars) and hypoxic (diagonally striped bars) at P11 and (B) at P18 (N = 3, N = 4 per group, respectively). (C) Density of apoptotic cells (number of cells per mm^3) in the neurogenic areas of control (open bars) and hypoxic (diagonally striped bars) at P11 and (D) at P18 (N = 4 per group). (E) Number of NeuN-positive neurons in the cerebral cortex and (F) cortical volume of control and hypoxic mice at P11, P18, and P49 (N = 4 for each group) *$P < 0.05$, **$P < 0.005$, comparing normoxia versus hypoxia at each age by Student's t test.

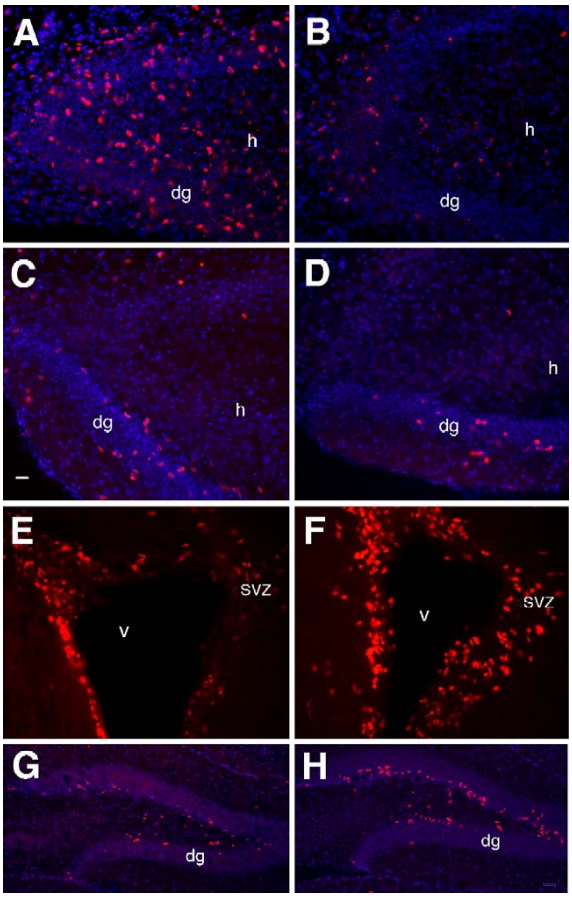

Fig. 4. Cell proliferation is decreased during hypoxia and increased after the cessation of the insult. (A, C, E, G) Normoxic and (B, D, F, H) hypoxic brains (coronal sections). DAPI (blue) and BrdU (red) at P4 (A–B), P11 (C–D), and P18 (E–H). DG, dentate gyrus; SVZ, subventricular zone; V, ventricle. Scale bar = 20 Am in A–F; 40 Am in G, H.

To test if perinatal hypoxia influenced the rate of cell death, we immunostained brain sections for the active form of caspase-3, an enzyme which triggers most forms of apoptosis. Although on average hypoxic brains had an increased density of cells expressing active caspase-3, this was statistically significant only in the hippocampal DG at P18 (Figs. 3C,D). These data suggest that apoptosis is most likely enhanced by perinatal hypoxia, however, because of the transient nature of apoptotic cells, the magnitude of this phenomenon was difficult to appreciate with current techniques.

Proliferation of astroglial cells in the SVZ after hypoxic rearing

To examine ways in which the brain undergoes self-repair after the chronic insult, we assessed cell proliferation within the two classic neurogenic regions of the postnatal mammalian brain, the SVZ and DG. After 24h of hypoxia, the density of proliferative cells was decreased in both the DG (Figs. 4A,B) and the SVZ (data not shown). This decrease in cell proliferation in hypoxic mice was also observed at P11 but was not as drastic at P4 (Figs. 4C,D). Unbiased estimates of the number of proliferative cells at P11

revealed that the decrease was significant in the DG but did not reach statistical significance in the SVZ due to a large variability in the response to hypoxia in different animals (Fig. 3A). These data suggest that hypoxia decreases cell proliferation in the SVZ and DG and that this acute effect diminishes as the hypoxia enters a chronic stage.

When hypoxic mice were allowed to recover for 7 days (P18) under normoxic conditions, there was an increase in the number of proliferative cells as compared to controls, both in the SVZ (Figs. 4E,F) and DG (Figs. 4G,H). Unbiased counts of BrdU-positive cells confirmed that the total number of BrdU-labeled cells was increased in both neurogenic regions, particularly in the SVZ (Figs. 3B and 5A,B). This increase was mostly attributable to the increased density of BrdU-positive cells with only a small increase in SVZ volume (average volume was 0.079 mm3 in hypoxic compared to 0.062 mm3 in normoxic mice). Very few BrdU-positive cells were present in the parenchyma of the brain outside the SVZ, DG, and rostral migratory stream (RMS). These results suggest that cell proliferation is enhanced during the recovery in the SVZ and DG.

To characterize these progenitors, we used antibodies to GLAST and BLBP, proteins expressed by radial glia–astrocyte cells in the VZ during embryogenesis (Edwards et al., 1990; Feng et al., 1994; Shibata et al., 1997). The SVZ of P18 hypoxic mouse brains showed an increased density of GLAST+ cells compared to age-matched controls (Figs. 5AV,BV). Similar increases were found using Vimentin . The neurogenic zones of hypoxic mice were also notable for increased in BLBP immunoreactivity (Figs. 5CV,DV). Furthermore, an increased number of both GLAST- and BLBP-immunoreactive cells incorporated a short pulse of BrdU in hypoxic-reared animals, both in the SVZ and DG (Figs. 5AW,BW and data not shown). The density of cells expressing

GFAP immunoreactivity was not changed, however, progenitor cells co-localizing BLBP and GFAP immunoreactivities were increased in hypoxic-reared mice (Fig. 5, compare CW with DW, arrows). These results indicate that an increased number of cells of the astroglial lineage are proliferating in the neurogenic zones after hypoxia.

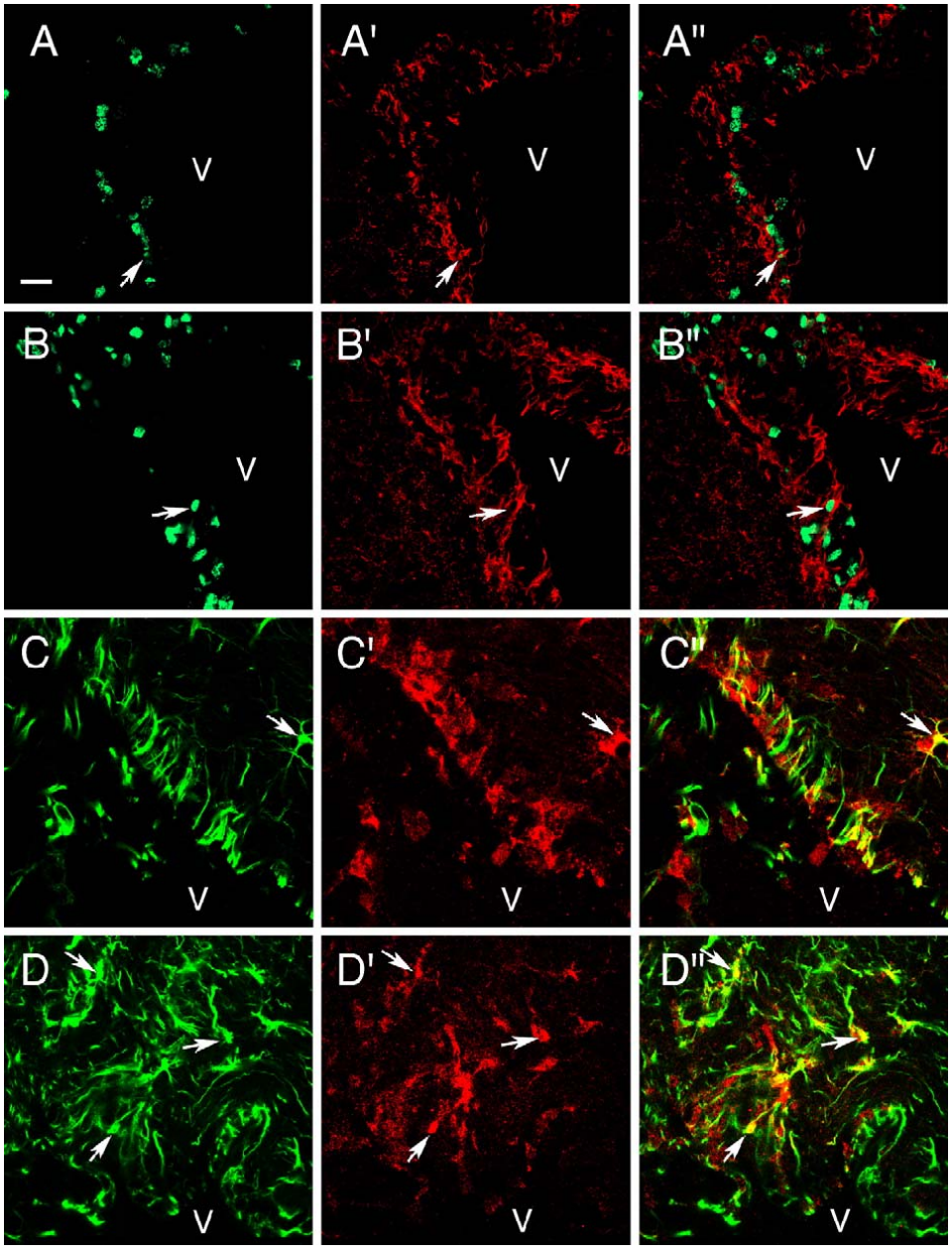

Figure 5. Characterization of proliferative cells in the neurogenic zones of P18 mice after hypoxic insult. (A and C) normoxic and (B and D) hypoxic brains (coronal sections). (A and B) Confocal images of BrdU (green) and GLAST (red) in the SVZ. (C and D) Confocal images of GFAP (green) and BLBP (red) in the SVZ. V, ventricle. Scale bar = 20 Am in A and B and 13 Am in C and D.

Migration of neuroblasts from the SVZ to the cerebral cortex

Astroglial cells give rise to neuroblasts, which migrate to the OB or DG via the RMS. To investigate whether the increased proliferation of astroglial cells resulted in an increased production of cells of the neuronal lineage, we immunostained sections for Mash1, PSA-NCAM, DLX-2, and Dcx. These proteins are transiently expressed by newly generated neurons, although Mash1 and DLX2 have also been associated with oligodendrocytes progenitors (Marshall and Goldman, 2002; Parras et al., 2004). PSA-NCAM-positive neuroblasts were restricted to the SVZ and the RMS (Doetsch et al., 1997). A subset of the PSA-NCAM cells co-expressed Mash1 (Figs. 6G,H, arrow-heads); yet, as cells began to migrate from the SVZ, they no longer expressed both markers and were either PSA-NCAM or Mash1 immunoreactive (Figs. 6G,H, arrows). We found a small percent of Mash1+ neuroblasts detached from the main stream of migrating cells in the RMS and changed their course from an anterior to a dorsal direction, penetrating the subcortical white matter and entering the inferior cortical layers (Figs. 6A–D, arrows). During this migration into the cortex, Mash1+ neuroblasts were closely apposed to GFAP+ astroglial cells in the subcortical white matter (Figs. 6A–D, arrowheads). Upon entering the cerebral cortex (Figs. 6A–D, marked by a dashed line), Mash1+ cells appeared detached from astrocytes (Figs. 6A–D, arrows) and soon afterwards Mash1 expression was apparently down-regulated. Likewise, PSA-NCAM-positive cells were detected changing trajectory to migrate dorsally. Among those neuroblasts that traveled dorsally, most were Mash1+, however, a few also expressed PSA-NCAM and DLX2 immunoreactivities, except that these proteins were more rapidly down-regulated before entering the cortical plate (Figs. 6G,H and I,J).

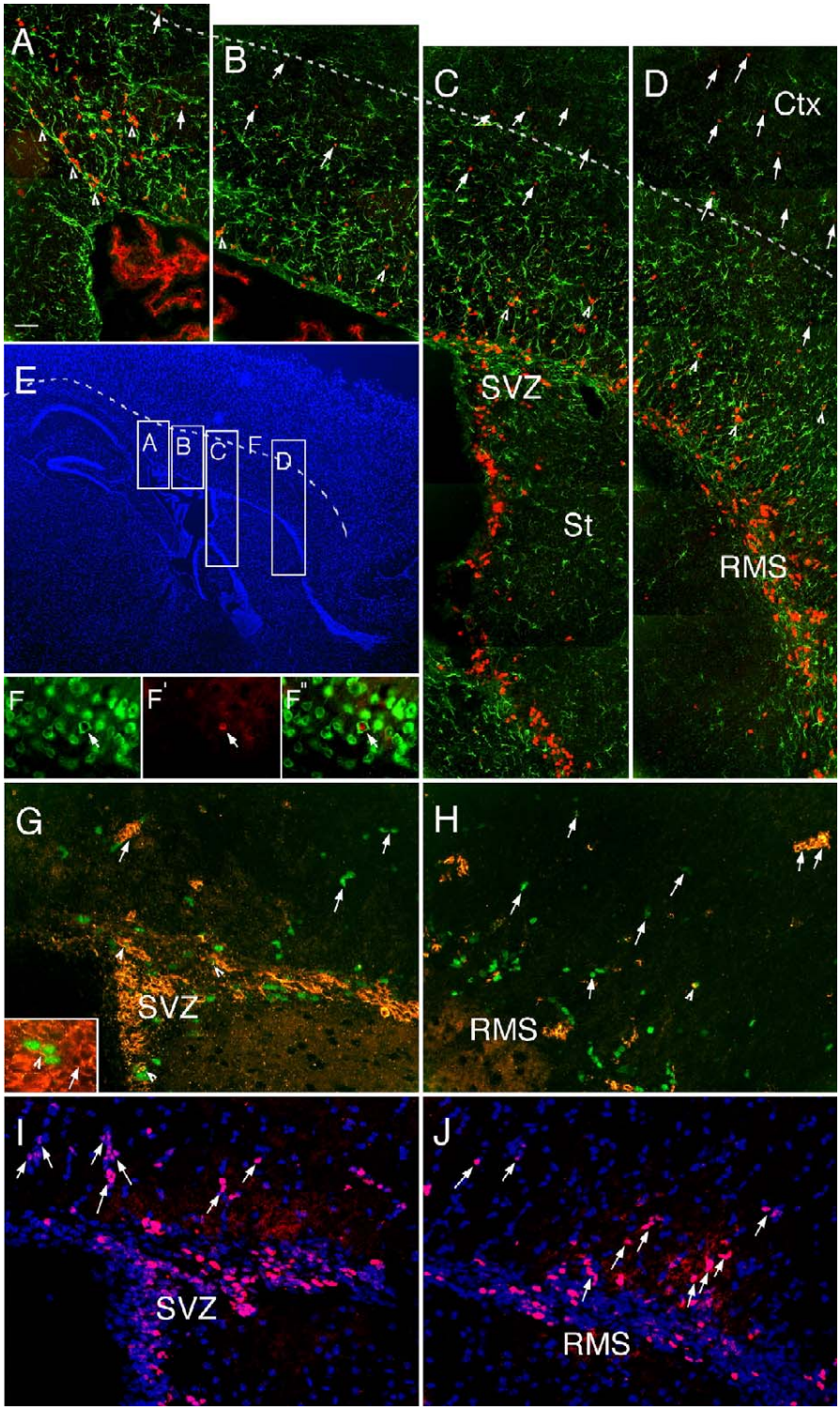

Figure 6. Migration of neuroblasts from the SVZ to the inferior cortical layers in the hypoxic brain at P29. Images are sagittal section from hypoxic-reared mice. (A–D) Mash1 (red) and GFAP (green) immunoreactivity. Arrowheads indicate Mash1 neuroblasts attached to GFAP astrocytes, whereas arrows indicate detached Mash1 cells. (E) DAPI image showing location of panels (A–F). (F–F'') NeuN (F, green), BrdU (F', red) and merged image (F'') in the inferior cortical layer. (G and H) Mash1 (green) and PSA NCAM (orange) showing co-localization and migration patterns in theSVZ and RMS. Arrow - heads show co-localized cells, whereas arrows indicate distinct neuronal subsets. (I and J) DLX-2 (red) and DAPI (blue). St, Striatum; RMS, Rostral Migratory Stream; Ctx, Cortex. Scale bar = 50 Am in A–D, 10 Am F–F" and 25 Am in G–J.

To confirm this phenomenon, we immunostained sections with Dcx, an established marker for migrating young cortical neurons (Bai et al., 2003). A similar migratory pattern from the SVZ and RMS to the subcortical white matter was observed

for Dcx+ neurons. This phenomenon of dorsal migration was observed in both hypoxic and normoxic mice at P23–29 (Fig. 6 shows hypoxic-reared mice). These data suggest the possible mechanism for replacing the cortical neurons lost due to chronic hypoxia.

To investigate the time required for this neuronal migration from the SVZ to the cerebral cortex, we labeled precursor cells with BrdU between P16-18 and allowed them to differentiate for 5 or 11 days (P23 and P29, respectively). The generation of new cortical neurons was confirmed using antibodies to the Hu protein, which is present in immature neurons (Gultekin et al., 2000; Pincus et al., 1998). Several Brd/Hu double-labeled young neurons were identified in the inferior cortical layers, above the SVZ and RMS at P23. A few days later, at P29, BrdU/NeuN co-labeled neurons were identified in the inferior cortical layers (Fig. 6FW). Hence, the location of these newly born neurons is within the migratory streams visualized with previous neuroblast markers.

Differentiation of cells born during hypoxic recovery

Next we examined the fate of the cells proliferating at P18. BrdU injections were given at P16 for 54h, and BrdU+ cells were allowed 31 days to differentiate. We determined the phenotype of BrdU+ cells by double-labeling with the oligodendrocyte marker Rip, the astrocyte marker GFAP, or the mature neuronal marker NeuN. The proportion of BrdU+ cells that acquired oligodendroglial, astroglial, or neuronal cell fates was ascertained by examining at least 100 randomly sampled cells (Fig. 7A). In normoxic animals, the largest percentage of newly generated cells (42.8%) became oligodendrocytes, while 35.5% became mature astrocytes and 9.2% differentiated into neurons. These percentages did not significantly differ in hypoxic animals (Fig. 7A).

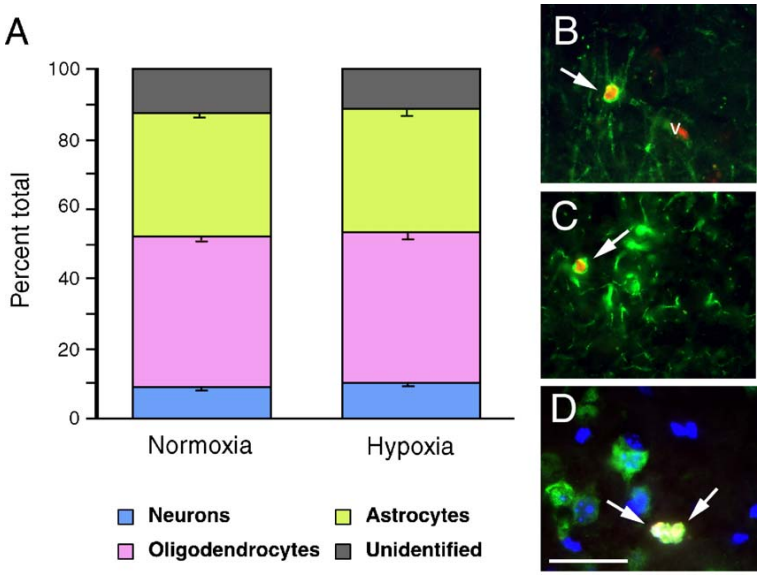

Figure 7. Phenotypic characterization of newly generated cortical cells. BrdU injected P16-18. Cells analyzed after 31 days (N=3 per condition). 100-200 BrdU+ cells were counted per brain. (A) Percent of Brdu+ cells co-localized with Rip, GFAP, or NeuN, markers for oligo-dendrocytes, astrocytes, and neurons, respectively. The majority differentiated into oligodend-rocytes (42.8%, normoxic and 43.5%, hypoxic). Rest became astrocytes (35.5, normoxic and 34.9%, hypoxic) or neurons (9.2%, normoxic and 10.2%, hypoxic). Unidentified cells accounted for 12.5% in normoxic and 11.4% in hypoxic. (B–D) Double immunostaining of representative cells. BrdU (B–D, red) and RIP (B, green), GFAP (C, green) and NeuN (D, green; DAPI, blue). Scale bar = 20 Am.

Because the generation of new cortical neurons in mice during the postnatal period has not been previously reported, we carried out more detailed analyses by labeling proliferating cells for either 16 h or 54 h and allowing them to survive for either 5, 31, or 60 days. BrdU/NeuN double-labeled cells were found in the cerebral cortex at 31 and 60 but not at 5 days. These cells did not appear to be satellite glia because the BrdU immunoreactivity was disseminated within the NeuN+ nucleus, as detected by confocal analyses in the z plane (Figs. 8A – F). BrdU/NeuN double-labeled neuronal cells varied in size and were apparently distributed throughout the cerebral cortex, with a preference for frontal regions (Figs. 8AW–DW). BrdU/Hu double-labeled neurons were also detected 31 days after BrdU incorporation (Fig. 8EW). Hu-positive cells tended to be smaller than NeuN, possibly because NeuN partly labels the neuronal cytoplasm while Hu is strictly nuclear. To determine if the newly generated neuronal cells were pyramidal neurons, we attempted to double-label BrdU-positive cells with antibodies to SMI-32, however, among more than 200 BrdU-positive cortical cells sampled, we could not detect any BrdU/SMI-32 double-labeled neurons after 31 or 60 days of

differentiation. This can in part be attributed to the fact that neuronal cell bodies are poorly stained for neurofilaments. Next, we examined whether the new neurons were expressing GABAergic markers. Among more than 200 BrdU+ cortical cells examined, 4 were double-stained with GABA antibodies (Fig. 8FW). However, no BrdU/parvalbumin double-stained neurons were detected.

Because our initial data suggested that cortical neuron loss was rapidly reversed during recovery, we compared the amount of neurogenesis in normoxic versus hypoxic animals. BrdU injections were given at P18 and cells were allowed to differentiate for 31 days. We then used stereological analyses in serial sections encompassing the whole brain to assess the total number of BrdU+ cells as well as the number that expressed NeuN in the cerebral cortex, basal ganglia, and DG of hypoxic and normoxic animals. We estimated that in the cerebral cortex of control mice, there were about 280,000 BrdU-immunoreactive cells and approximately 19,000 (or 6.8%) of these BrdU+ cells expressed the NeuN neuron marker (Table 2). In contrast, there were on average about 400,000 BrdU+ cells in the cortex of hypoxic mice, and approximately 40,000 of these cells (or 10%) were double-labeled with NeuN (Table 2). Hence, there were twice as many BrdU/NeuN-positive cells in the cerebral cortex of mice recovering from hypoxia. As expected, more than 60% of the newly generated cells in the DG were neurons, and this proportion was nearly equal in hypoxic and normoxic conditions (64.6% versus 67.3%, respectively; Table 2). On average, 30% more newly generated neurons were found in the DG of hypoxic-reared mice, however, the difference was not statistically significant (Table 2). In contrast, no BrdU/ NeuN double-stained cells could be detected in the basal ganglia under either hypoxic or normoxic rearing conditions (Table 2).

Mice recovering from perinatal hypoxia had twice as many newly generated cortical neurons with respect to normoxic controls

	Normoxia	Hypoxia	%
Cerebral cortex			
Total neurons (NeuN)	15,967,403 (±1,419,335)	14,215,905 (±479,818)	−11
Total BrdU-positive	283,817 (±107,721.8)	400,929 (±96,961.39)	+41.3
Total BrdU/NeuN	19,308 (±6,649)	40,043* (±5,468)	+107.4
Percent BrdU/NeuN	6.80%	9.99%	
Basal ganglia			
Total neurons (NeuN)	2,039,572 (±522,083)	2,035,003 (±281,535)	−0.2
Total BrdU-positive	48,953 (±10,916)	36,309 (±11,927)	−25.8
Total BrdU/NeuN	0	0	
Percent BrdU/NeuN	0	0	
Dentate gyrus			
Total neurons (NeuN)	588,590 (±105,280)	572,826 (±82,885)	−2.7
Total BrdU-positive	12,458 (±1,386)	16,837 (±3,963)	+35.2
Total BrdU/NeuN	8,386 (±1,060)	10,876 (±2,664)	+29.7
Percent BrdU/NeuN	67.3%	64.6%	

Table 2. Mice were exposed to chronic hypoxia from P3 to P11 or were kept under normoxic conditions. Proliferative cells were labeled by in vivo BrdU incorporation for 16h at P18. The total numbers of NeuN-immunostained neurons and of newly generated BrdU-labeled cells were estimated in brain regions of P49 mice by unbiased stereological analyses in serial sections. The number of BrdU/NeuN double-labeled cells represents the number of neurons that underwent the last mitosis at P18 during the 16h labeling period and survived until P49. N = 4 control and 4 hypoxic animals. Percent of BrdU/NeuN indicated the percentages of BrdU/NeuN double-labeled cells with respect to the total number of BrdU-labeled cells.
* $P < 0.05$, Student's t test.

Neurons can incorporate BrdU as a result of repairing their DNA, thus invalidating the assumption that BrdU was incorporated into cells undergoing S phase (Nowakowski et al., 1989). To address this issue, we performed a control experiment by administering an identical series of cumulative BrdU injections at P18 and sacrificing the animals 20 h later. Based on a time course performed in the hippocampal DG, BrdU-labeled cells begin to express NeuN after 3 days (Brandt et al., 2003). Thus, we assumed that 20h would not be enough time for S-phase cells to differentiate into NeuN + neurons and that BrdU/NeuN double-labeled cells at this short survival time would reflect the labeling due to neurons undergoing DNA repair. Indeed, confocal analyses demonstrated that few NeuN+ cortical neurons incorporated a very small amount of BrdU at the 20-h time point. If the 19,000 BrdU/NeuN double-immunoreactive cells detected at P49 in the normoxic brains were to be accounted for by this DNA repair

phenomenon, their number should have been the same as that obtained at P19. However, the total number of BrdU/NeuN double-stained cortical cells present at P19 was variable, estimated to be on average 3940 cells on the basis of counts obtained in three brains. Moreover, there was only a single spot of BrdU incorporation in the chromatin of BrdU-labeled neurons at P19, which is consistent with lower rates of DNA synthesis in DNA repair. In contrast, our estimation of BrdU double-labeled cells at P49 included only cells with extensive BrdU incorporation in their nuclei (Figs. 7 and 8), which is consistent with S-phase labeling. Together, these data suggest that the number and morphology of BrdU/NeuN double-stained cells found in the cerebral cortex of hypoxic and normoxic mice at P49 was not consistent with cells undergoing DNA repair and thus these double-stained cells likely derived from progenitors dividing at P18.

The recovery of cortical neurons after hypoxia requires Fgfr1

To determine the role that Fgfr1 plays in neurogenesis after hypoxia, Fgfr1 cKO mice (which lack the intact Fgfr1 gene in GFAP+ cells) (Ohkubo et al., 2004) were exposed to sublethal hypoxia (9.5–10.5% O_2) for 7d, from P3 to P10. After injury on P10, the hypoxic mice exhibited a decrease in cortical thickness (Fig. 9 A,B) and a significant 24% decrease in cortical volume (70.57 +/-2.54 mm^3 for normoxic vs 53.67 +/-2.21 mm^3 for hypoxic; $p < 0.05$). The number of NeuN+ neurons in the cerebral cortex, quantified by stereological analysis, declined from 10.2 +/-0.4 x 10^6 to 7.3 +/-0.8 x 10^6 cells ($p < 0.05$), revealing a 29% decrease compared with age-matched normoxic controls (Fig. 9 I, blue bars). To determine whether hypoxia decreased the number of excitatory neurons, sections were immunostained using antibodies to the transcription

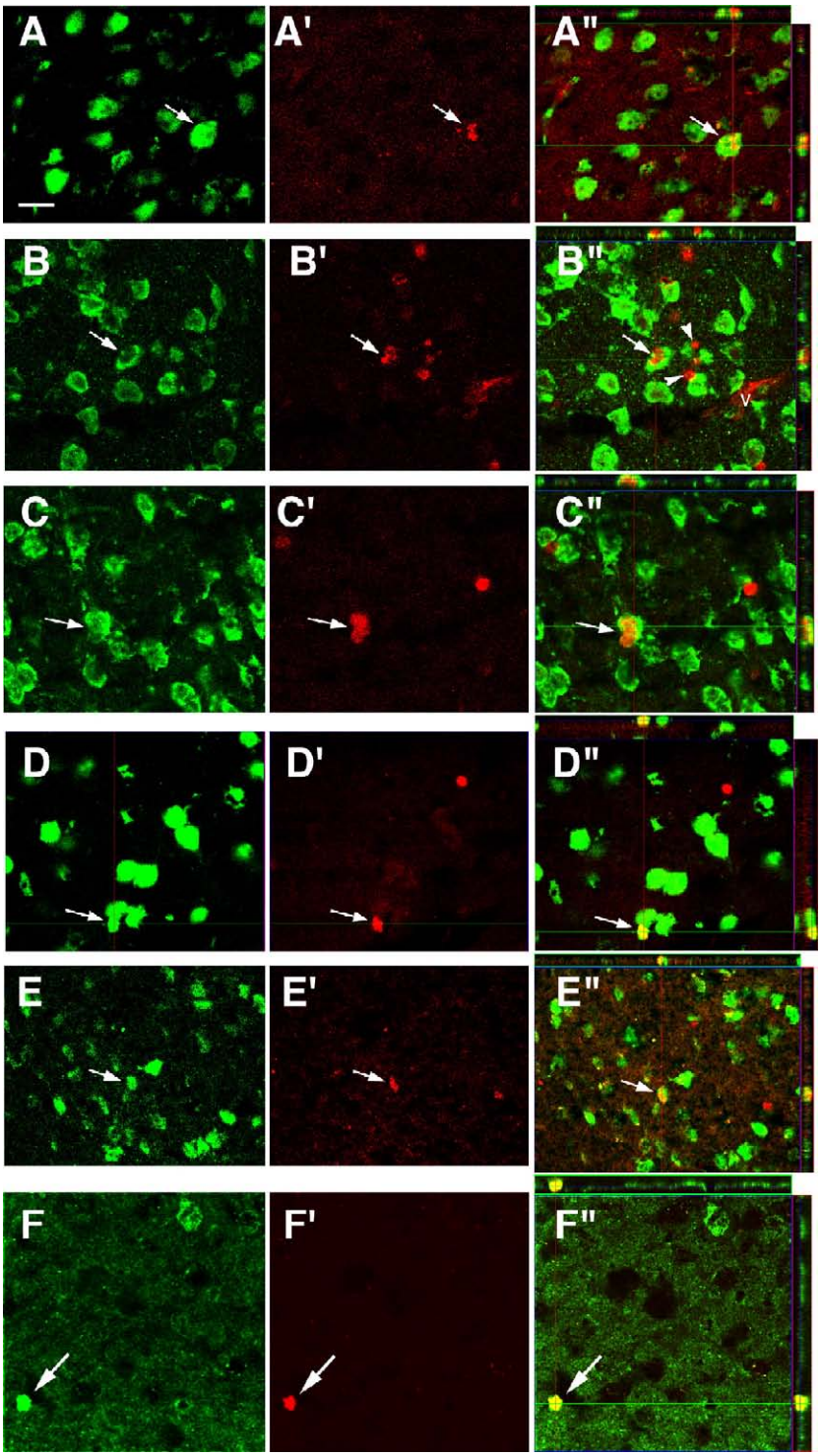

Fig. 8. Newly generated neurons in the cerebral cortex of P49 and P78 normoxic and hypoxic mice. Mice were subjected to hypoxia from P3 to P11, cumulatively treated with BrdU between P16 and P18, and allowed to survive until P49 (A–E) or P78 (F). (A–B) Normoxic and (C–F) Hypoxic. (A–F) Neuronal markers: (A–D) NeuN; (E) Hu; (F) GABA. (AV–FV) BrdU labeling; (AW–FW) merged confocal images (z-stack analysis in shown in side panels). Arrows indicate examples of newly generated cells, and arrowheads indicate examples of satellite glia. V = blood vessel. Scale bar = 20 Am.

factor Tbr1 and the neurofilament epitope SMI-32, which label subsets of cortical pyramidal neurons (Campbell et al., 1991; Hevner et al., 2006). Tbr1 regulates the differentiation of early born glutamatergic cortical neurons (Hevner et al., 2001). In the immature cortex, Tbr1 is expressed by pyramidal cells, in the subplate and in layer 1 Reelin+ cells. In adulthood, Tbr1 becomes progressively restricted to layer 6 pyramidal cells, although in rostral cortex it is expressed in layers 5 and 2/3 as well (Bulfone et al., 1995; Hevner et al., 2001, 2006). At P10, the number of Tbr1+ neurons in the cortex of hypoxic mice declined from 6.3 +/-0.4 x 10 to 4.4 +/-0.3 x 10 cells ($p < 0.05$), revealing a 31% statistically significant deficit in Tbr1+ cells in the supra- and infra-granular layers (Fig. 1A,B,J, blue bars). Total loss of Tbr1+ excitatory neurons (1.95 X 10^6 neurons) accounted for 67% of NeuN+ neurons lost (2.92 x 10^6) (Fig. 9, compare I,J). There was an even greater decrease (66%) in SMI-32+ neurons (Fig. 9 E,F,K, blue bars).

Previous findings link FGF to the development of excitatory neurons (Korada et al., 2002), Tbr1+ neurons (Shin et al., 2004) during embryogenesis. Fgfr1 continues to be expressed by cells of the postnatal SVZ and astrocytes throughout the brain, (see Supplemental Fig 1. and Fgfr1 BAC-EGFP transgenic mouse in Gensat Project, http://www.gensat.org/index.html). To investigate the role of Fgfr1 in recovery, the cKO were exposed to hypoxia. Notably, the Fgfr1 cKO mice did not exhibit any baseline defect in NeuN+, Tbr1+ or SMI-32+ cortical neuron number (Fig. 10 A,C,I–K), suggesting that in the absence of injury, Fgfr1 does not play a major role in cortical morphogenesis. Similar to wild-type mice, hypoxic Fgfr1 cKO mice suffered a 33%, 31%, and 70% loss of NeuN+, Tbr1+ andSMI-32+ cortical neurons, respectively (Fig.10 C,D,G,H,I–K). Hence, the absence of Fgfr1 did not worsen the neuronal loss caused by hypoxia.

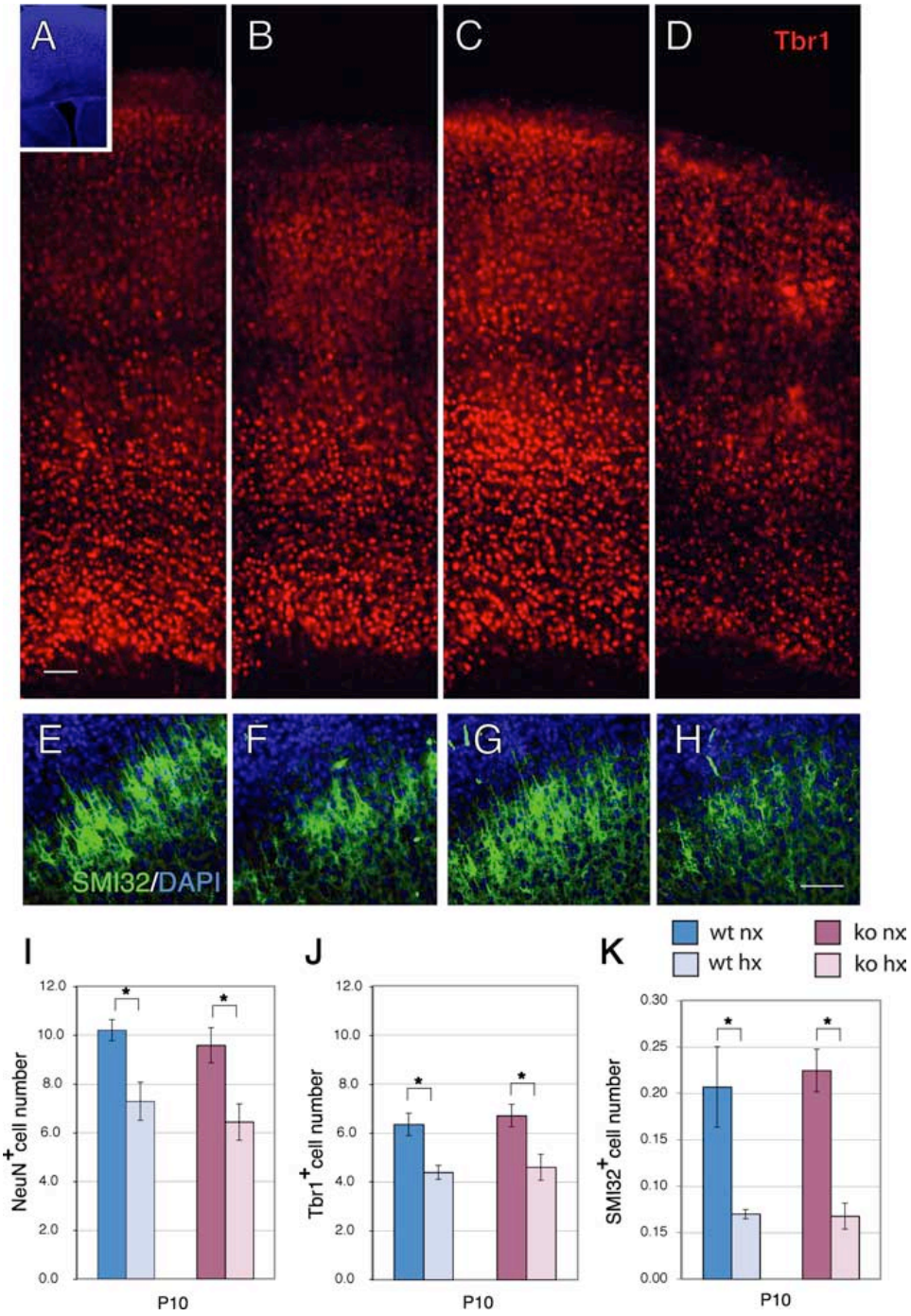

Figure 9. Cortical neuron number and thickness are decreased after exposure to hypoxia. A–D, Immunostaining for Tbr1 (red) in the cerebral cortex of wild-type (A, B) or Fgfr1 cKO mice (C, D) at P10 under normoxia (A, C) or after hypoxia from P3 to P10 (B,D). Inset shows DAPI low magnification. Each panel is the composite of four 20× images demonstrating the entire extent of the cerebral cortex. E–H, SMI-32 (green) and DAPI (blue) stained cortices of wild-type (E,F) or Fgfr1 cKO mice (G,H) at P10 under normoxia (E, G) or after hypoxia from P3 to P10 (F, H). Scale bars, 100 µm. I–K, Total number of NeuN (I), Tbr1 (J) and SMI-32 (K) immunoreactive neurons in the cerebral cortex by stereological analyses in wild-type (blue bars) and Fgfr1 cKO (red bars) mice. Values are expressed in 106 units. N = 3 for each group. *p<0.05 by ANOVA with Sheffe post hoc test.

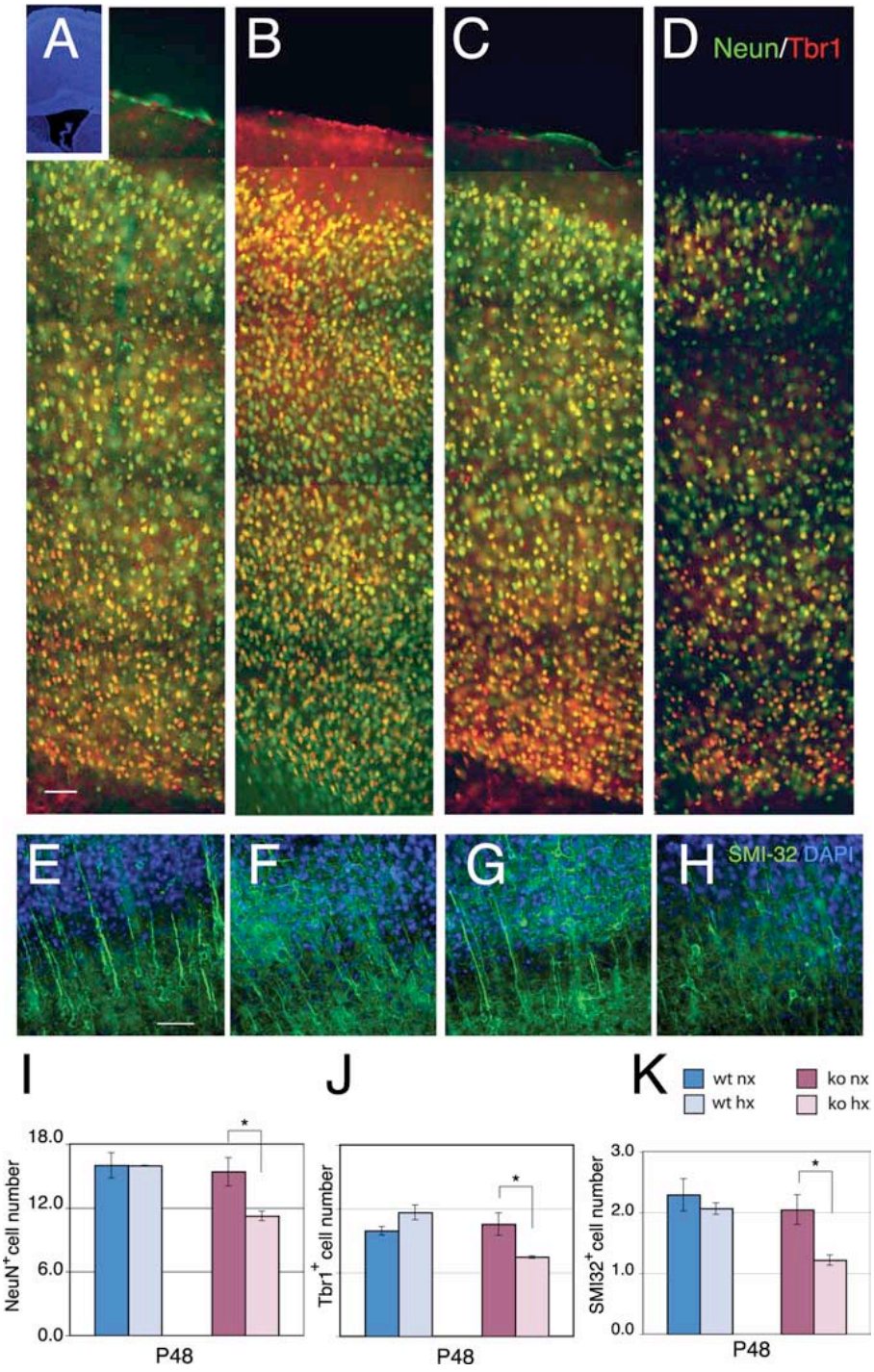

Figure 10. Neuron numbers recover in hypoxic wild-type mice but not in Fgfr1 cKO mice. A–D, Double immunostaining for NeuN (green) and Tbr1 (red) in the P48 cerebral cortex of wild-type (A, B) or Fgfr1 cKO mice (C, D) under normoxia (A, C) or after hypoxia (B, D). Inset shows DAPI low magnification. Each panel is the composite of five 20× images. E–H, SMI-32- (green) and DAPI- (blue) stained cortices of wild-type (E, F) or Fgfr1 cKO mice (G, H) at P48 under normoxia (E, G) or after hypoxia from P3 to P10 (F, H). Scale bars, 100 µm. I–K, Total number of NeuN (I), Tbr1 (J) and SMI-32 (K) immunoreactive neurons in the cerebral cortex by stereological analyses in wild-type (blue bars) and Fgfr1 cKO (red bars) mice. Values expressed in 106 units. N = 3 for each group. *$p < 0.05$ by ANOVA with Sheffe post hoc test.

Although there was a residual 17% decrease in cortical volume (103.49 +/-4.16 mm^3 for normoxic vs 85.75 +/-1.29 mm^3 for hypoxic; $p < 0.05$) the initial deficit in NeuN+ neurons was no longer present in the hypoxic wild-type mice at P48, after 4 weeks of recovery (Fig. 12 A,B,I), confirming our previous results in mice of pure C57BL background (Fagel et al., 2006). To determine the proportion of neuronal subtypes in normoxic and hypoxic mice at this stage, we estimated the number of cortical excitatory neurons expressing Tbr1 and SMI-32 and that of inhibitory neurons expressing PV and CR by stereological analyses. Hypoxic mice showed no significant difference in the total number of Tbr1+ and SMI-32+ cortical neurons compared with normoxic controls at P48 (Fig. 10 A,B,E,F,J,K, blue bars). In contrast, total number of PV+ and CR+ interneurons was significantly decreased by 32 and 43%, respectively, in hypoxia-reared mice ($p < 0.01$) (Fig. 11 A,B,E,F,M,N, blue bars). Given that PV and CR cells comprise a much smaller population, compared with Tbr1+ excitatory neurons, no changes in the total number of cortical neurons were detected in hypoxic mice, as shown by the analysis of NeuN (Fig. 10 I). However, the proportion of excitatory and inhibitory neurons changed substantially in the cerebral cortex at 4 weeks post injury. The ratio between Tbr1+ and the sum of PV+ and CR+ neurons in the normoxic cortex was ~7 to 1, whereas this ratio was 12 to 1 in the hypoxic cortex. In sum, the data show no evidence for long-term neuronal loss but a substantial imbalance in the proportion of excitatory versus inhibitory neurons after hypoxia.

In normoxic conditions, no difference in NeuN+, Tbr1+ or SMI-32+ neuron number was detected between Fgfr1 cKO mice and wild-type mice (Fig. 10 I–K);

however, these mice exhibited a basal 32% deficit of PV+ interneurons (Fig. 11 M,N) as described previously (Muller-Smith et al., 2008). This 32% loss of interneurons was not accompanied by a detectable decrease in total neurons, presumably because PV+ interneurons comprise a relatively small subset of total cortical neurons (i.e., 1.07 +/- 0.06 million cells for PV+ neurons vs 15.98 +/-1.19 million cells for NeuN+ neurons).

The long-term response to hypoxia was significantly different in Fgfr1 cKO and wild-type mice. First, hypoxic Fgfr1 cKO mice continued to show statistically significant deficits of 27%, 29% and 37% in NeuN+, Tbr1+ and SMI-32+ cortical neurons, respectively ($p<0.05$) (Fig. 2 C,D,G,H,I–K, red bars). Second, Fgfr1 cKO mice, which had a baseline 32% decrease in PV+ interneurons, showed an additional decrease of 39% and a 53% in PV+ and CR+ cells, respectively, after hypoxia (Fig. 3 C,D,M,N).

Hypoxia-induced cortical and olfactory bulb neurogenesis requires Fgfr1

We next investigated the possible mechanisms underlying the recovery of Tbr1+ cortical neuron number after hypoxia in wild-type mice and the absence of this recovery in Fgfr1 cKO mice. We first examined whether progenitors, labeled with BrdU 1 week after hypoxia, can differentiate into Tbr1+ neurons. Proliferative cells were labeled with four cumulative BrdU injections administered at P17 to incorporate BrdU in the whole population of constitutively proliferating cells and their fate was analyzed 31 days later at P48. Our estimate suggested the presence of 54,800 NeuN+ /BrdU+ and 19,200 Tbr1+/ BrdU+ cortical neurons in normoxic cortices. These cells had a relatively small nucleus and were often present in doublets, suggesting that they were the product of a

recent cell division (Fig. 12 A–Q). In hypoxic mice, NeuN+/BrdU+ cortical neurons at P48 were estimated to be 114,040, while Tbr1+/BrdU+ neurons were estimated to be 72,225, which represent a 108% and a 280% increase, respectively, compared with normoxic controls (Fig. 12 R,S, blue bars). Tbr1+/BrdU+ neurons accounted for just 35% of all NeuN+/BrdU+ neurons in normoxic mice, whereas they accounted for 63% of all NeuN+/BrdU+ neurons in hypoxic mice. The data suggest that proliferative progenitors give rise to new neurons in the immature cerebral cortex, that this phenomenon is increased by previous exposure to hypoxic insult, and that the proportion of progenitors giving rise to Tbr1+ neurons is higher in hypoxic-reared mice.

These results indicate that hypoxic Fgfr1 cKO mice were unable to upregulate the rate of cortical neurogenesis 1 week after the insult (Fig. 12 R,S, red bars). Hypoxic Fgfr1 cKO showed the same amount of newly generated neurons as their normoxic counterparts, although it remains possible that the Fgfr1 cKO have a smaller neurogenetic response that reaches completion before P17, that is insufficient to reverse the deficits. We also noticed that in the absence of injury, the Fgfr1 cKO mice showed a 48% basal deficit in NeuN+/BrdU+ cortical neurons, but not in Tbr1+/BrdU+ neurons, compared with wild-type littermates (Fig. 12 R,S). Hence, whereas Tbr1+/BrdU + neurons accounted for just 35% of NeuN+/BrdU+ neurons in normoxic wild-type mice, the Tbr1+/BrdU+ cells accounted for 95% of NeuN+/BrdU+ neurons in normoxic Fgfr1 cKO mice (Fig. 12 R,S). The data indicate that Fgfr1 is required for the production of non-Tbr1+ neurons under normoxic conditions, as well as for the production of both non-Tbr1+ and Tbr1+ neurons after injury.

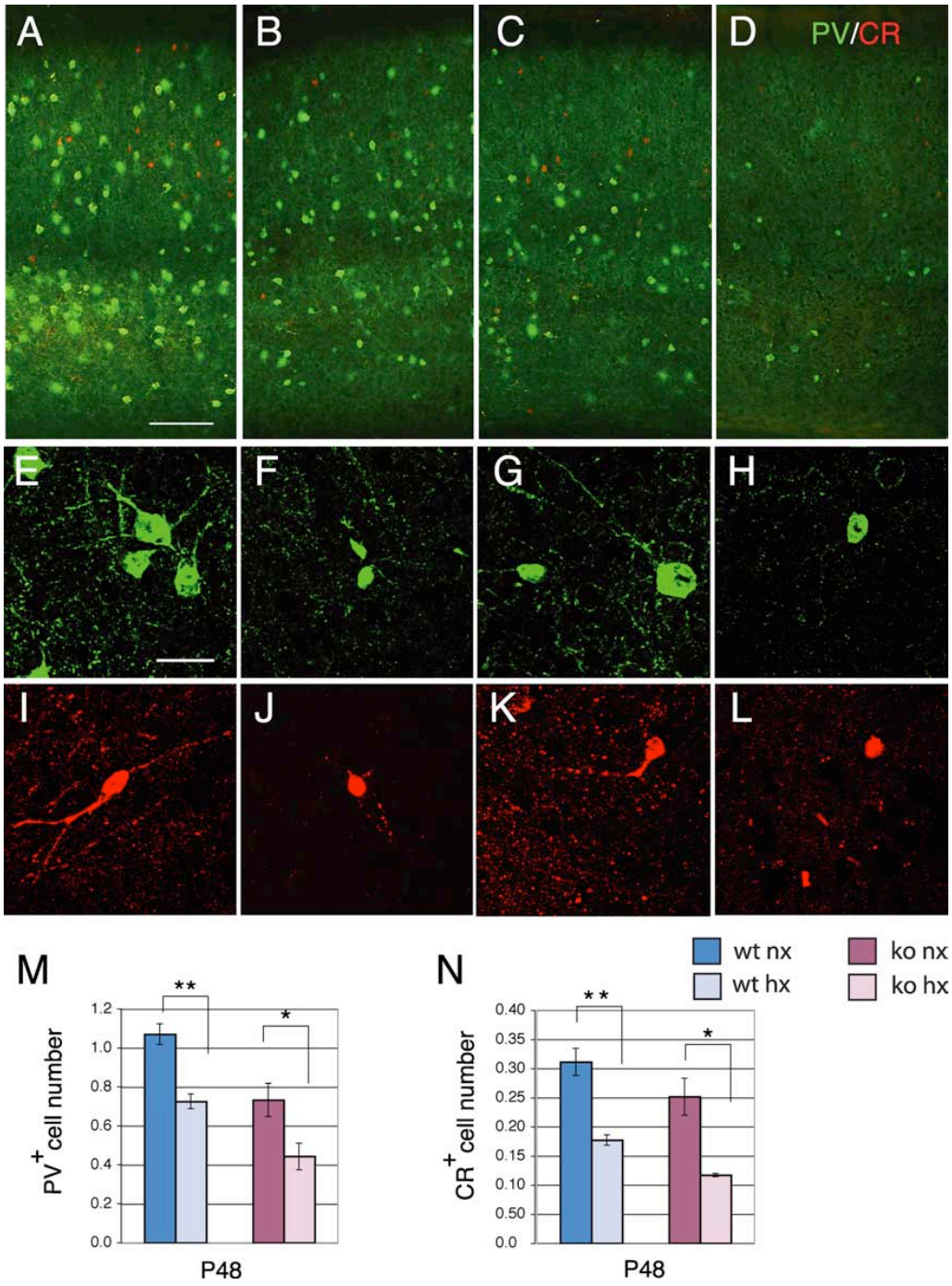

Figure 11. Cortical interneuron number is decreased at P48 in both hypoxic wild-type and Fgfr1 cKO mice. A–D, Double immunostaining for PV (green) and CR (red) in the P48 cerebral cortex of wild-type (A, B) or Fgfr1 cKO mice (C, D) under normoxia (A, C) or after hypoxia (B, D). Each panel is the composite of two images to show all layers of the cerebral cortex. E–L, Individual PV+ and CR+ neurons in hypoxia-reared mice (F, J, H, L) and their normoxic counterparts (E, I, G, K). Scale bars: (A–D) 100 µm; (E–L) 10 µm. M, N, Total number of PV (M) and CR (N) immunoreactive neurons by stereological analyses in wild-type (blue bars) and Fgfr1 cKO (red bars) mice. Values are expressed in 10^6 units. N = 3 for each group. *$p < 0.05$ and **$p < 0.01$ by ANOVA with Sheffe post hoc test.

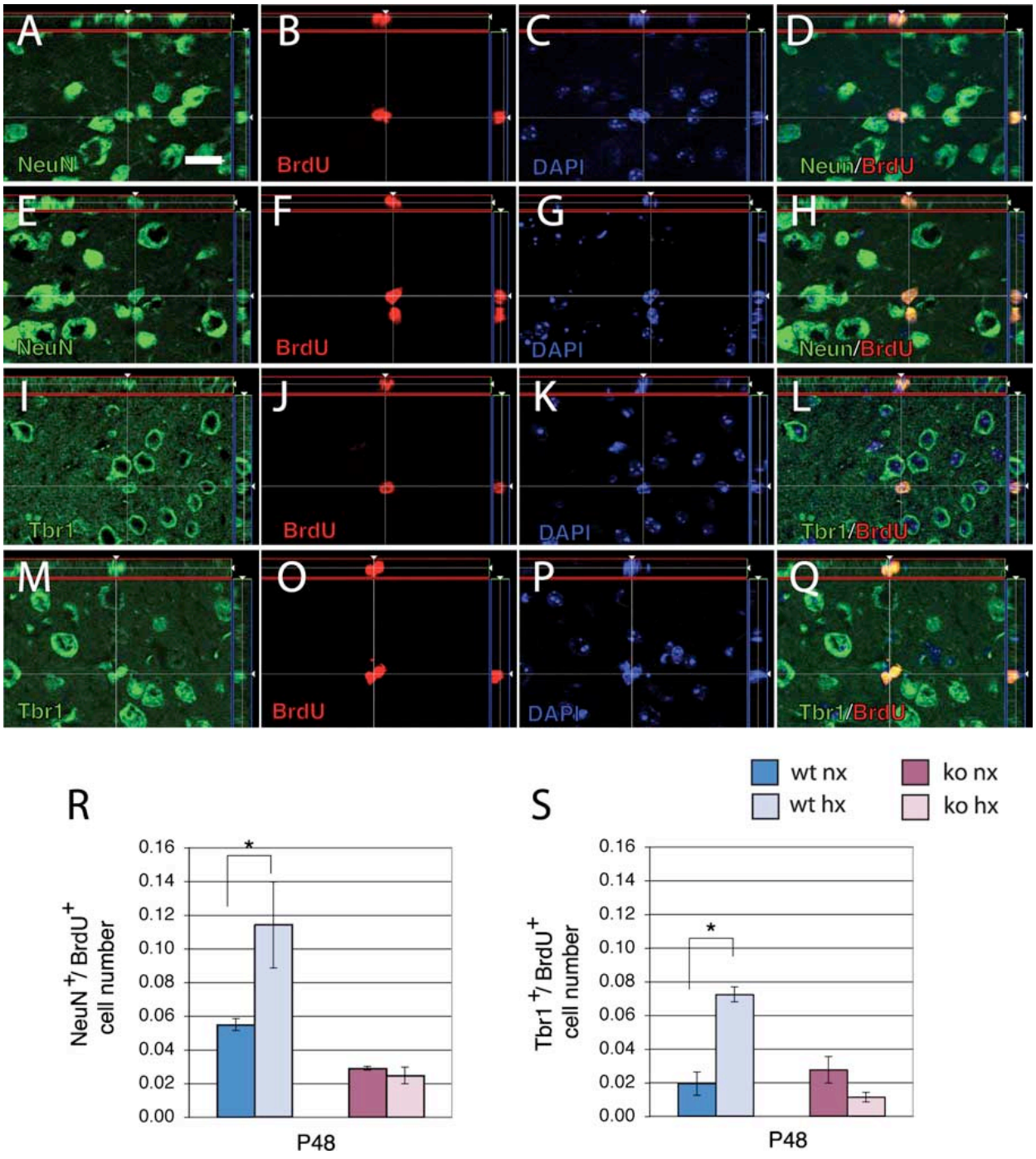

Figure 12. Newly generated NeuN+ and Tbr1+ cortical neurons are increased at P48 in hypoxic wild-type but not in Fgfr1 cKO mice. A–Q, Apotome 1 µm single slices of BrdU staining in the P48 cerebral cortex double-immunostained with NeuN (A–H) or Tbr1 (I–Q). BrdU was injected at P17 and analysis performed at P48. The image analyses on the z-axis are shown in the side panels. NeuN (A, E), Tbr1 (I, M), BrdU (B,F,J,O), DAPI (C,G,K,P), and merged images (D,H,L,Q). BrdU colocalization is observed in neurons born at P17 in normoxic (A–D, I–L) and hypoxic cortex (E–H, M–Q). R, S, Total number of NeuN/Brdu (R) and Tbr1/Brdu (S) double-labeled neurons in the cerebral cortex by stereological analyses in wild-type (blue bars) and Fgfr1 cKO (red bars). Scale bar, 10 µm. Values are expressed in 10^6 units. N = 3 for each group. *$p < 0.05$ by ANOVA with Sheffe post hoc test.

Condition	NeuN density (cells/mm^3)	BrdU/NeuN density (cells/mm^3)	Ratio BrdU/ NeuN to total NeuN
Normoxic WT	547,795 ± 62,476	56,388 ± 9895	0.102 ± 0.01
Hypoxic WT	634,300 ± 58,263[a]	189,575 ± 20,981**	0.303 ± 0.04**
Normoxic *Fgfr1 cKO*	620,820 ± 206,132	61,181 ± 30,414	0.088 ± 0.02
Hypoxic *Fgfr1 cKO*	658,110 ± 30,250[a]	104,210 ± 4605[a]	0.160 ± 0.01*

Table 3. Mice were exposed to chronic hypoxia from P3 to P10 or were kept under normoxic conditions. Proliferative cells were labeled by in vivo BrdU incorporation for 14h at P17. The density of NeuN+ neurons and that of newly generated BrdU+/NeuN+ labeled neurons was estimated in the granular layer of the OB at P48 by unbiased stereological analyses. The ratio between newly generated BrdU+/NeuN+ neurons to total NeuN+ neurons is shown in the last column. N = 3 control and 4 hypoxic animals. *$p < 0.05$ and **$p < 0.005$ by Student's t test comparing hypoxic versus normoxic mice. WT, Wild type. [a] Not statistically different from normoxic mice.

Neurogenesis was also assessed in the OB at P48, after the cumulative BrdU injections at P17. The results indicate that while the total density of NeuN+/BrdU+ cells in the granular layer of the OB increased by 335% in hypoxic wild-type mice ($p < 0.005$), the hypoxic cKO did not show any significant increase compared with their normoxic counterparts (Table 3). The proportion of neurons that were newly generated from these BrdU-labeled cells with respect to all neurons in the OB was 30% in hypoxic wild-type compared with 10% in the normoxic mice, a difference which was highly significant ($p < 0.005$). Interestingly, the hypoxic cKO did show a modest increase in percentage of OB neurons that arose from BrdU-labeled precursors compared with their normoxic counterparts (from 8% to 16%, $p < 0.05$) yet smaller than wild type (Table 3).

Fgfr1-dependent proliferation of neural progenitors in the reactive period

Confirming data obtained in rat tissue (Ganat et al., 2002), we observed that after cessation of the hypoxic insult, there was a 60% increase in Fgfr-1 immunoreactivity in

the SVZ of wild-type mice along with an increase in immunoreactivity for Sox2, Pax6 and Tbr2 which are transcription factors expressed by neural stem and precursor cells in the SVZ. As expected, in Fgfr-1 cKO mice, the Fgfr-1 protein was not detected in the SVZ neuroepithelium, and the upregulation in Sox2+, Pax6+ and Tbr2+ cells induced by chronic hypoxia was attenuated (Supplemental Fig. 1).

To assess whether Fgfr1 expression in neural progenitors played a role in their proliferation or survival, BrdU was administered shortly before sacrifice at both P10 and P17. At P10, the hypoxic wild-type and Fgfr1 cKO showed a 30 and 45% loss of BrdU+ cells in the SVZ, respectively, compared with their normoxic counterparts (Fig. 13 I). To understand whether some of the stem/progenitor cells may have undergone apoptosis during the exposure to hypoxia, we analyzed the SVZ for activated Caspase-3, a marker for cells undergoing apoptosis, immediately after cessation of injury. In both wild-type and Fgfr1 cKO mice, hypoxia caused a near doubling in number of apoptotic cells in the SVZ at P10 (Fig. 13 E–H, J). These data suggest that hypoxia decreases cell proliferation in the SVZ by promoting progenitor apoptosis, and that Fgfr1 does not play a major role in stem/ progenitor cell proliferation or survival in normal development, neither it changes their susceptibility to die in response to injury.

Short-term BrdU incorporation assays were then performed 1 week later, at P17, to assess cell proliferation in the posthypoxia reactive phase in both wild-type and Fgfr1 cKO mice. In the absence of injury, the Fgfr1 cKO mice did not show any difference in cell proliferation compared with the wild-type littermates. After injury, the wild-type hypoxic mice showed an 85% increase in BrdU+ cells in the SVZ compared with their

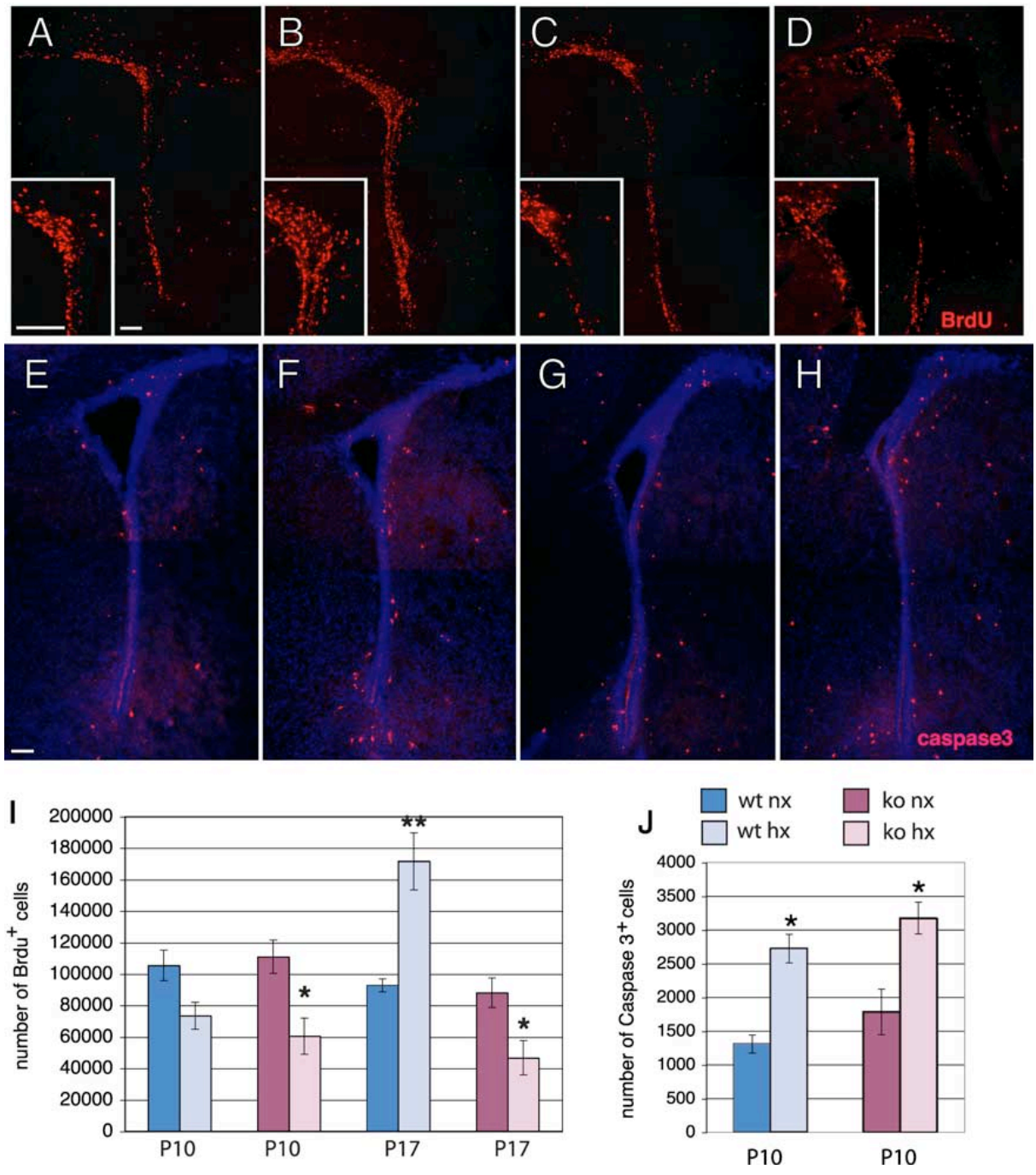

Figure 13. Increase in proliferation in the SVZ during recovery requires Fgfr1. A–D, BrdU immunostaining in the SVZ at P17 of wild-type (A, B) or Fgfr1 cKO mice (C, D) under normoxia (A, C) or after hypoxia (B, D). Insets show high magnifications. E–H, Caspase-3 immunostaining in the SVZ at P10 of wild-type (E, F) or Fgfr1 cKO (G, H) mice under normoxia (E, G) or after hypoxia (F,H). I,J, Total number of BrdU+ cells (I) at P10 and P17 and caspase-3+ cells (J) at P10 in the SVZ by stereological analyses in wild-type (blue bars) and Fgfr1 cKO (red bars). Scale bar, 100 μm. N=3 for each group. *$p < 0.05$ and **$p < 0.01$ by ANOVA with Sheffe post hoc test.

normoxic counterparts (Fig. 13 A, B,I). In Fgfr1 cKO mice, however the number of BrdU + cells at P17 further declined to 47% below that of their normoxic counterparts (Fig. 13 C,D,I). Our data demonstrate that while basal cell proliferation in non-hypoxic mice was not dependent upon Fgfr1 functioning, Fgfr1 was clearly required for the surge in SVZ cell proliferation after hypoxia, suggesting that this receptor may be an essential component of the hypoxia-induced proliferative response. Combined, these data indicate that after exposure to hypoxia, Fgfr1 may be critical for inducing cell proliferation in normally quiescent astroglial stem/progenitor cells in the SVZ.

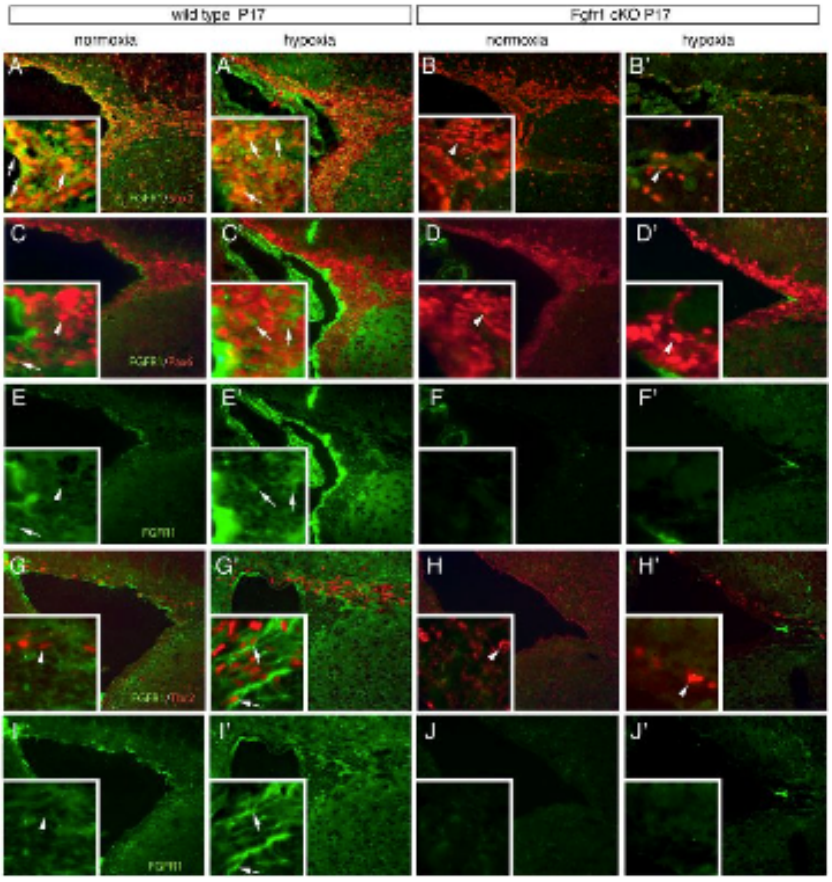

Supplemental Figure 1. Fgfr1 in stem cells and progenitor cells of the SVZ. Immunocytochemistry for Fgfr1 (green) together with Sox2 (A-B'), Pax6 (C-D') or Tbr2 (G-H') (all in red) in P17 mice. E-F' and I-J' show green channel alone corresponding to the Fgfr1 immunostaining in C-D' and G-H', respectively. Note the apparent hypoxia-induced upregulation of Fgfr1 in the SVZ of wild type mice and the absence of Fgfr1 expression in the SVZ of cKO mice, with the exception of some staining in the endothelium and ependyma. Also note that the hypoxia-induced upregulation of Sox2+, Pax6+ and Tbr2+ cells was attenuated in Fgfr1 cKO hypoxic mice. Arrowheads point to precursor cells devoid of Fgfr1 expression

Discussion

We report that chronic sublethal hypoxia in newborn mice produces an initial 30% deficit in cortical neurons, two-thirds of which are excitatory neurons expressing the transcription factor Tbr1. Over the ensuing 4 weeks in normoxic conditions, the deficit in neuron number recovers, such that neither NeuN+, Tbr1+ nor SMI-32+ neurons are decreased in the cortex of hypoxic-reared mice at P48. However, there is an enduring loss in PV+ and CR+ inhibitory interneurons in the hypoxic mice, which creates an imbalance between excitatory and inhibitory neurons in the hypoxic cortex. Disrupting the Fgfr1 gene in GFAP+ cells of the developing dorsal telencephalon (including cortical radial glial cells and all their progeny) does not alter the initial loss of cortical neurons but precludes the recovery of NeuN+ , Tbr1+ and SMI-32+ neuron number in the cerebral cortex. Hypoxic exposure increases cell proliferation and the generation of $Tbr1^+$ cortical excitatory neurons and that of OB granular neurons, processes that are absent or greatly attenuated in Fgfr1 cKO mice. Thus the juvenile cerebral cortex possesses an unsuspected capacity to recover from a postnatal hypoxic insult, which depends on the functioning of critical signaling systems, i.e., Fgfr1. As rodents are born earlier in the developmental program compared with primates, this hypoxic protocol models injury during late human gestation and the neonatal period, as it typically occurs in prematurely born infants, as well as ensuing recovery processes in human childhood.

The reconstitution of excitatory cortical neuron number after the hypoxic insult is surprising, as excitatory neurons were previously thought to be generated only during embryogenesis. It is possible that the initial loss may be less profound than what is revealed by NeuN and Tbr1 neuron counts, since some of the damaged neurons may not express neuronal markers and may subsequently recover. We cannot exclude that our assessment of the initial extent of neuron loss may be an over-estimate due to such a process. Nevertheless, we consistently observed corresponding decreases in neuron number, brain weight and cortical thickness in the hypoxia-reared mice, in at least two genetic backgrounds (Fig. 1 A, B) (Fagel et al., 2006; Fagel et al., 2009. Further, we show that cell death is twofold higher in hypoxic brains, indicating probable cell losses.

We noticed that in the current mixed strain of mice, the total number of cortical neurons increases by almost 6 million cells between P10 and P48 in normoxic mice (compare Figs. 9 and 10), suggesting a high degree of cellular plasticity even in the normal juvenile mouse cerebral cortex. This is consistent with recent unbiased stereological studies suggesting that total neuron number progressively increases in the early postnatal rodent cerebral cortex, albeit to varying degrees in different mouse strains, and that there is delayed acquisition of cortical neuron features over the postnatal period (Lyck et al., 2007). Thus, part of the postnatal increase in the number of cortical neurons may be attributable to a progressive accumulation of neuronal antigens, such as NeuN and SMI-32. Nonetheless, using BrdU birthdating assays, we report that part of the increase in cortical neuron number is attributable to the addition of new cortical neurons in the third postnatal week after birth. These BrdU+ neurons are unlikely to be the result of neuronal repair or impending neuronal death (Kuan et al.,

2004), because apoptotic cells would have been already eliminated 4 weeks after BrdU incorporation. Furthermore, we have previously shown (Zheng et al., 2004) that neurons strongly immunolabeled with BrdU do not reflect ongoing DNA repair at these dosages of the nucleotide. Also supporting the idea of a hypoxia-induced proliferative effect as opposed to DNA repair are the increase in total number of cells and volume of the SVZ observed by us (Fagel et al., 2006; Fagel et. al., 2009) and others (Plane et al., 2004) and the absence of a correlation between apoptotic cell number and BrdU+ cells in the SVZ at different survival times after the hypoxic insult (Fagel et al., 2006). Finally, we have detected postnatal addition of neurons to the immature cerebral cortex using genetic fate mapping, which allowed us to mark with B-galactosidase GFAP+ neural stem cells in vivo (Ganat et al., 2006).

In wild-type hypoxic mice, BrdU/NeuN and BrdU/Tbr1 double-positive neurons increased twofold and threefold, respectively, compared with age-matched normoxic mice. This can be attributed to hypoxia increasing the proliferation or survival of progenitors, particularly those committed to a Tbr1+ phenotype. Alternatively, hypoxia may increase the capacity of newly born, post-mitotic neurons to differentiate and survive in the cortical environment. The first hypothesis is supported by a nearly twofold increase in cell proliferation in the SVZ in hypoxia-exposed mice compared with age-matched controls (Fagel et al., 2006; Fagel et al., 2009), and by previous reports suggesting that hypoxia-ischemia increases cell proliferation in the brain (Plane et al., 2004; Ong et al., 2005; Park et al., 2006; Zhao et al., 2008). Furthermore, neural precursor cells expressing the neurogenic transcription factors Sox2, Pax6 and Tbr2 in the SVZ appear to increase after hypoxia. In contrast, in the hypoxic Fgfr1 cKO mice,

the SVZ proliferative response is absent, and the increase in Sox2-, Pax6- and Tbr2-immunoreactive cells is attenuated. These data highlight the central role of Fgfr1, whose expression is restricted to glial cells (Belluardo et al., 1997; Vaccarino et al., 2001; Ganat et al., 2002) (Gensat Project: http://www.gensat.org/ index.html) in promoting neuronal progenitor proliferation after postnatal hypoxic injury.

Dividing precursors in the SVZ and rostral migratory stream generate neurons for the OB (Luskin, 1993; Alvarez-Buylla and Garcia-Verdugo, 2002; Aguirre and Gallo, 2004; Hack et al., 2005) and Fgf2 (a ligand for Fgfr1) is required for the maintenance of this proliferating cell pool (Zheng et al., 2004). Consistently, Fgfr1 cKO mice are unable to properly upregulate OB neurogenesis in response to hypoxia. The failure to observe a statistically significant increase in density of NeuN+/BrdU+ cells in the OB of Fgfr1 cKO mice may be attributable in part to the large variability between animals; however, the mean increase in NeuN+/BrdU+ cells from normoxic to hypoxic cKO (70%) is much less than that observed wild-type mice (236%), suggesting that if there was an increase in OB neurogenesis in the hypoxic cKO, it was more modest. Thus, the absence of a post-hypoxic proliferative response in the SVZ of Fgfr1 cKO mice likely underlies their decreased ability to regenerate OB neurons, although other events unrelated to Fgfr1, such as cell survival, may play a compensatory role in regulating OB neurogenesis.

Fgfr1 cKO mice exposed to hypoxia suffer the same level of apoptosis and initial cortical cell loss as wild-type mice, but fail to recover, exhibiting a persistent 31–33% deficit in total neurons and excitatory cortical neurons 5 weeks later. Furthermore, in the absence of Fgfr1, the generation of cortical neurons from BrdU-labeled cells is not

upregulated in the recovery period. These data suggest that Fgfr1 is not involved in neuroprotection after injury, but rather, in the regenerative and reactive response. At present, we do not understand whether the unresponsiveness of SVZ progenitors underlies the failure to boost cortical neurogenesis in the Fgfr1 cKO mice, as BrdU birthdating cannot reveal whether the progenitors that generate cortical neurons arise from the SVZ. It is possible that increased generation of NeuN+ and Tbr1+ cortical neurons occurs from proliferative progenitors in the cortex itself, as mature cortical astrocytes may re-enter the cell cycle and acquire multipotency in vitro after cortical injury (Buffo et al., 2008). Furthermore, although Fgfr1 is clearly required for the hypoxia-induced increase in proliferation in the SVZ, it may play an additional role in fostering neuronal repair in the brain parenchyma, and thus contribute to the recovery of neurons damaged by hypoxia. For example, the loss of Fgfr-1 may alter the ability of astroglial cells to regulate the exchange of molecules involved in energy regulation, or secrete trophic factors that might affect neuronal progenitors in a paracrine manner.

In contrast to the recovery of Tbr1+ neuron number, hypoxia caused an enduring deficit in inhibitory cortical PV+ and CR+ interneurons (32 and 43%, respectively). We could not estimate the extent of the initial loss of PV+ and CR+ inhibitory neurons after hypoxia, since at P11 the maturation of calcium-binding protein immunoreactivities is not yet complete. Hence, we cannot ascertain whether the significant decreases in PV+ and CR+ cells present in hypoxia-reared mice represent an enduring loss, a failure to properly mature, or a progressive demise.

In conclusion, chronic neonatal hypoxia induces a chain of linked events, beginning with the upregulation of Fgfr1 expression in neural stem cells, which in turn increases the generation of Tbr2+ and Pax6+ proliferative neuronal progenitors. This work provides the first demonstration that after neonatal chronic hypoxic injury, the initial loss of SMI-32 and Tbr1-expressing excitatory cortical neurons spontaneously recovers in the juvenile cerebral cortex. Furthermore, glial Fgfr1 plays a central role in driving this recovery, as both the increased neurogenesis and reconstitution of normal cortical neuron number are not seen in mice that lack Fgfr1 in GFAP+ cells. This reconstituted neuron number is stable 9 weeks after neonatal hypoxic injury (Fagel et al., 2006). In contrast, we show that PV and CR inhibitory interneurons do not show a comparable degree of recovery, resulting in marked imbalance in excitatory/inhibitory neurons in the hypoxic cerebral cortex.

References

Aguirre A, Gallo V (2004) Postnatal neurogenesis and gliogenesis in the olfactory bulb from NG2-expressing progenitors of the subventricular zone. J Neurosci 24:10530 – 10541.

Allin M, Henderson M, Suckling J, Nosarti C, Rushe T, Fearon P, Stewart AL, Bullmore ET, Rifkin L, Murray R (2004) Effects of very low birth weight on brain structure in adulthood. Dev Med Child Neurol 46:46 –53.

Allin, M., Nosarti, C., Narberhaus, A., Walshe, M., Frearson, S., Kalpakidou, A., Wyatt, J., Rifkin, L., Murray, R., 2007. Growth of the corpus callosum in adolescents born preterm. Arch. Pediatr. Adolesc. Med. 161, 1183–1189.

Als, H., Behrman, R., Checchia, P., Denne, S., Dennery, P., Hall, C.B., Martin, R., Panitch, H., Schmidt, B., Stevenson, D.K., Vila, L., 2007. Preemie abandonment? Multi-disciplinary experts consider how to best meet preemies needs at "preterm infants: a collaborative approach to specialized care" roundtable. Mod. Healthc. 37, 17–24.

Als, H., Duffy, F.H., McAnulty, G.B., Rivkin, M.J., Vajapeyam, S., Mulkern, R.V., Warfield, S.K., Huppi, P.S., Butler, S.C., Conneman, N., Fischer, C., Eichenwald, E.C., 2004. Early experience alters brain function and structure. Pediatrics 113, 846–857.

Altman, J., Das, G.D., 1965. Autoradiographic and histological evidence of postnatal hippocampal neurogenesis in rats. J. Comp. Neurol. 124, 319 – 335.

Alvarez-Buylla A, Garcia-Verdugo JM (2002) Neurogenesis in adult sub- ventricular zone. J Neurosci 22:629 – 634.

Androutsellis-Theotokis A, Leker RR, Soldner F, Hoeppner DJ, Ravin R, Poser SW, Rueger MA, Bae SK, Kittappa R, McKay RD (2006) Notch signaling regulates stem cell numbers in vitro and in vivo. Nature 442:823– 826.

Arvidsson A, Collin T, Kirik D, Kokaia Z, Lindvall O (2002) Neuronal replacement from endogenous precursors in the adult brain after stroke. Nat Med 8:963–970.

Bai, J., Ramos, R.L., Ackman, J.B., Thomas, A.M., Lee, R.V., LoTurco, J.J., 2003. RNAi reveals doublecortin is required for radial migration in rat neocortex. Nat. Neurosci. 6, 1277–1283.

Belluardo N, Wu G, Mudo G, Hansson AC, Pettersson R, Fuxe K (1997) Comparative localization of fibroblast growth factor receptor-1, -2, and -3 mRNAs in the rat brain: in situ hybridization analysis. J Comp Neurol 379:226 –246.

Buffo A, Rite I, Tripathi P, Lepier A, Colak D, Horn AP, Mori T, Götz M (2008) Origin and progeny of reactive gliosis: a source of multipotent cells in the injured brain. Proc Natl Acad Sci U S A 105:3581–3586.

Bulfone A, Smiga SM, Shimamura K, Peterson A, Puelles L, Rubenstein JLR (1995) T-brain-1:a homolog of brachyury whose expression defines molecularly distinct domains within the cerebral cortex. Neuron 15:63–78.
Chahboune, H., Ment, L.R., Stewart, W.B., Rothman, D.L., Vaccarino, F.M., Hyder, F., Schwartz, M.L., in press. Hypoxic injury during neonatal development in murine brain: correlation between in vivo DTI findings and behavioral assessment. Cereb. Cortex.

Campbell MJ,Hof PR, Morrison JH (1991) A subpopulation of cortical neurons is distinguished by somatodendritic distribution of neurofilament protein. Brain Res 539:133–136.

Chiang, M.C., Barysheva, M., Shattuck, D.W., Lee, A.D., Madsen, S.K., Avedissian, C., Klunder, A.D., Toga, A.W., McMahon, K.L., de Zubicaray, G.I., Wright, M.J., Srivastava, A., Balov, N., Thompson, P.M., 2009. Genetics of brain fiber archi- tecture and intellectual performance. J. Neurosci. 29, 2212–2224.

Constable, R.T., Ment, L.R., Vohr, B.R., Kesler, S.R., Fulbright, R.K., Lacadie, C., Delancy, S., Katz, K.H., Schneider, K.C., Schafer, R.J., Makuch, R.W., Reiss, A.R., 2008. Prematurely born children demonstrate white matter microstructural differ- ences at 12 years of age, relative to term control subjects: an investigation of group and gender effects. Pediatrics 121, 306–316.

Dell'Anna, M.E., Calzolari, S., Molinari, M., Iuvone, L., Calimici, R., 1991. Neonatal anoxia induces transitory hyperactivity, permanent spatial memory deficits and CA1 cell density reduction in developing rats. Behav. Brain Res. 45, 125– 134.

Doetsch, F., Garcia-Verdugo, J.M., Alvarez-Buylla, A., 1997. Cellular composition and three-dimensional organization of the subventricular germinal zone in the adult mammalian brain. J. Neurosci. 17, 5046 – 5061.

Doetsch, F., Caille, I., Lim, D.A., Garcia-Verdugo, J.M., Alvarez-Buylla, A., 1999. Subventricular zone astrocytes are neural stem cells in the adult mammalian brain. Cell 97, 703–716.

Dono R, Texido G, Dussel R, Ehmke H, Zeller R (1998) Impaired cerebral cortex development and blood pressure regulation in Fgf2-deficient mice. EMBO J 17:4213–4225.

Douglas, R.M., Miyasaka, N., Takahashi, K., Latuszek-Barrantes, A., Haddad, G.G., Hetherington, H.P., 2007. Chronic intermittent but not constant hypoxia decreases NAA/Cr ratios in neonatal mouse hippocampus and thalamus. Am. J. Physiol. Regul. Integr. Comp. Physiol. 292, R1254–1259.

Fagel DM, Ganat Y, Silbereis J, Ebbitt T, Stewart W, Zhang H, Ment LR, Vaccarino FM (2006) Cortical neurogenesis enhanced by chronic perinatal hypoxia. Exp Neurol 199:77–91.

Fagel, D.M., Ganat, Y., Cheng, E., Silbereis, J., Ohkubo, Y., Ment, L.R., Vaccarino, F.M., 2009. Fgfr1 is required for cortical regeneration and repair after perinatal hypoxia. J. Neurosci. 29, 1202–1211.

Fanaroff, A.A., Stoll, B.J., Wright, L.L., Carlo, W.A., Ehrenkranz, R.A., Stark, A.R., Bauer, C.R., Donovan, E.F., Korones, S.B., Laptook, A.R., Lemons, J.A., Oh, W., Papile, L.A., Shankaran, S., Stevenson, D.K., Tyson, J.E., Poole, W.K., NICHD Neonatal Research Network, 2007. Trends in neonatal morbidity and mortality for very low birthweight infants. Am. J. Obstet. Gynecol. 196, 147.e1–147.e8.

Fearon P, O'Connell P, Frangou S, Aquino P, Nosarti C, Allin M, Taylor M, Stewart A, Rifkin L, Murray R (2004) Brain volumes in adult survivors of very low birth weight: a sibling-controlled study. Pediatrics 114:367–371.

Felling, R.J., Snyder, M.J., Romanko, M.J., Rothstein, R.P., Ziegler, A.N., Yang, Z., Givogri, M.I., Bongarzone, E.R., Levison, S.W., 2006. Neural stem/progenitor cells participate in the regenerative response to perinatal hypoxia/ischemia. J. Neurosci. 26, 4359–4369.

Feng, L., Hatten, M.E., Heintz, N., 1994. Brain lipid-binding protein (BLBP): a novel signaling system in the developing mammalian CNS. Neuron 12, 895–908.

Gage, F.H., 1998. Stem cells of the central nervous system. Curr. Opin. Neurobiol. 8, 671–676.

Ganat Y, Soni S, Chacon M, Schwartz ML, Vaccarino FM (2002) Chronic hypoxia up-regulates fibroblast growth factor ligands in the perinatal brain and induces fibroblast growth factor-responsive radial glial cells in the sub-ependymal zone. Neuroscience 112:977–991.

Ganat YM, Silbereis J, Cave C, Ngu H, Anderson GM, Ohkubo Y, Ment LR, Vaccarino FM (2006) Early postnatal astroglial cells produce multilineage precursors and neural stem cells in vivo. J Neurosci 26:8609 – 8621.

Gimenez, M., Junque, C., Narberhaus, A., Botet, F., Bargallo, N., Mercader, J.M., 2006a. Correlations of thalamic reductions with verbal fluency impairment in those born prematurely. Neuroreport 17, 463–466.

Gimenez, M., Junque, C., Vendrell, P., Narberhaus, A., Bargallo, N., Botet, F., Mercader, J.M., 2006b. Abnormal orbitofrontal development due to prematurity. Neurol- ogy 67, 1818–1822.

Gultekin, S.H., Rosai, J., Demopoulos, A., Graus, Y.F., Posner, J.B., Dalmau, J., Rosenblum, M.K., 2000. Hu immunolabeling as a marker of neural and neuroendocrine differentiation in normal and neoplastic human tissues: assessment using a recombinant anti-Hu Fab fragment. Int. J. Surg. Pathol. 8, 109–117.

Hack M, Flannery DJ, Schluchter M, Cartar L, Borawski E, Klein N (2002) Outcomes in young adulthood for very-low-birth-weight infants. N Engl J Med 346:149 –157.

Hack MA, Saghatelyan A, de Chevigny A, Pfeifer A, Ashery-Padan R, Lledo PM, Gotz M (2005) Neuronal fate determinants of adult olfactory bulb neurogenesis. Nat Neurosci 8:865– 872.

Hayes NL , Nowakowski RS (2000) Exploiting the dynamics of S-phase tracers in developing brain: interkinetic nuclear migration for cells entering versus leaving the S-phase. Dev Neurosci 22:44 –55.

Hevner RF, Shi L, Justice N, Hsueh Y, Sheng M, Smiga S, Bulfone A, Goffinet AM, Campagnoni AT, Rubenstein JL (2001) Tbr1 regulates differentiation of the preplate and layer 6. Neuron 29:353–366.

Hevner RF, Hodge RD, Daza RA, Englund C (2006) Transcription factors in glutamatergic neurogenesis: conserved programs in neocortex, cerebellum, and adult hippocampus. Neurosci Res 55:223–233.

Hoehn BD, Palmer TD, Steinberg GK (2005) Neurogenesis in rats after focal cerebral ischemia is enhanced by indomethacin. Stroke 36:2718 –2724.

Inder, T.E., Warfield, S.K., Wang, H., Huppi, P.S., Volpe, J.J., 2005a. Abnormal cerebral structure is present at term in premature infants. Pediatrics 115, 286–294.

Korada S, Zheng W, Basilico C, Schwartz ML, Vaccarino FM (2002) Fgf2 is necessary for the growth of glutamate projection neurons in the anterior neocortex. J Neurosci 22:863– 875.

Kornack DR, Rakic P (2001) Cell proliferation without neurogenesis in adult primate neocortex. Science 294:2127–2130.

Kuan CY, Schloemer AJ, Lu A, Burns KA, Weng WL, Williams MT, Strauss KI, Vorhees CV, Flavell RA, Davis RJ, Sharp FR, Rakic P (2004) Hypoxia-ischemia induces DNA synthesis without cell proliferation in dying neurons in adult rodent brain. J Neurosci 24:10763–10772.

Lois, C., Alvarez-Buylla, A., 1993. Proliferating subventricular zone cells in the adult mammalian forebrain can differentiate into neurons and glia. Proc. Natl. Acad. Sci. U. S. A. 90, 2074–2077.

Luskin MB (1993) Restricted proliferation and migration of postnatally generated neurons derived from the forebrain ventricular zone. Neuron 11:173–189.

Lyck L, Krøigård T, Finsen B (2007) Unbiased cell quantification reveals a continued increase in the number of neocortical neurons during early postnatal development in mice. Eur J Neurosci 26:1749 –1764.

Magavi SS, Macklis JD (2002) Induction of neuronal type-specific neurogenesis in the cerebral cortex of adult mice: manipulation of neural precursors in situ. Brain Res Dev Brain Res 134:57–76.

Ment LR, Vohr B, Allan W, Katz KH, Schneider KC, Westerveld M, Duncan CC,MakuchRW (2003) Change in cognitive function over time in very low-birth-weight infants. Jama 289:705–711.

Ment LR, Allan WC, Makuch RW, Vohr B (2005) Grade 3 to 4 intraventricular hemorrhage and Bayley scores predict outcome. Pediatrics 116:1597– 1598; author reply 1598.

Ment, L.R., Kesler, S., Vohr, B., Katz, K.H., Baumgartner, H., Schneider, K.C., Delancy, S., Silbereis, J., Duncan, C.C., Constable, R.T., Makuch, R.W., Reiss, A.L., 2009. Longitudinal brain volume changes in preterm and term control subjects during late childhood and adolescence. Pediatrics 123, 503–511.

Monfils MH, Driscoll I, Kamitakahara H, Wilson B, Flynn C, Teskey GC, Kleim JA, Kolb B (2006) Fgf2-induced cell proliferation stimulates anatomical, neurophysiological and functional recovery from neonatal motor cortex injury. Eur J Neurosci 24:739 –749.

Muller Smith K, Fagel DM, Stevens HE, Rabenstein RL, Maragnoli ME, Ohkubo Y, Picciotto MR, Schwartz ML, Vaccarino FM (2008) Deficiency in inhibitory cortical interneurons associates with hyperactivity in fibroblast growth factor receptor 1 mutant mice. Biol Psychiatry 63:953–962.

Nakatomi H, Kuriu T, Okabe S, Yamamoto S, Hatano O, Kawahara N, Tamura A, Kirino T, Nakafuku M (2002) Regeneration of hippocampal pyramidal neurons after ischemic brain injury by recruitment of endogenous neural precursors. Cell 110:429 – 441.

Nosarti, C., Giouroukou, E., Healy, E., Rifkin, L., Walshe, M., Reichenberg, A., Chitnis, X., Williams, S.C., Murray, R.M., 2008. Grey and white matter distribution in very preterm adolescents mediates neurodevelopmental outcome. Brain 131, 205–217.

Nowakowski RS, Lewin SB, Miller MW (1989) Bromodeoxyuridineimmu-nohistochemical determination of the lengths of the cell cycle and the DNA-synthetic phase for an anatomically defined population. J Neurocytol 18:311–318.

Nyakas, C., Buwalda, B., Luiten, P.G., 1996. Hypoxia and brain development. Prog. Neurobiol. 49, 1–51.

Ohkubo Y, Uchida AO, Shin D, Partanen J, Vaccarino FM (2004) Fibroblast growth factor receptor 1 is required for the proliferation of hippocampal progenitor cells and for hippocampal growth in mouse. J Neurosci 24:6057– 6069.

Ong J, Plane JM, Parent JM, Silverstein FS (2005) Hypoxic-ischemic injury stimulates subventricular zone proliferation and neurogenesis in the neonatal rat. Pediatr Res 58:600 – 606.

Ortega S, Ittmann M, Tsang SH, Ehrlich M, Basilico C (1998) Neuronal defects and delayed wound healing in mice lacking fibroblast growth factor 2. Proc Natl Acad Sci U S A 95:5672–5677.

Palmer, T.D., Markakis, E.A., Willhoite, A.R., Safar, F., Gage, F.H., 1999. Fibroblast growth factor-2 activates a latent neurogenic program in neural stem cells from diverse regions of the adult CNS. J. Neurosci. 19, 8487–8497.

Parent JM, Vexler ZS, Gong C, Derugin N, Ferriero DM (2002) Rat forebrain neurogenesis and striatal neuron replacement after focal stroke. Ann Neurol 52:802–813.

Park KI, Hack MA, Ourednik J, Yandava B, Flax JD, Stieg PE, Gullans S, Jensen FE, Sidman RL, Ourednik V, Snyder EY (2006) Acute injury directs the migration, proliferation, and differentiation of solid organ stem cells: evidence from the effect of hypoxia-ischemia in the CNS on clonal “reporter” neural stem cells. Exp Neurol 199:156 –178.

Peterson, B.S., Anderson, A.W., Ehrenkranz, R., Staib, L.H., Tageldin, M., Colson, E., Gore, J.C., Duncan, C.C., Makuch, R., Ment, L.R., 2003. Regional brain volumes and their later neurodevelopmental correlates in term and preterm infants. Pedia- trics 111, 939–948.

Pincus, D.W., Keyoung, H.M., Harrison-Restelli, C., Goodman, R.R., Fraser, R.A., Edgar, M., Sakakibara, S., Okano, H., Nedergaard, M., Goldman, S.A., 1998. Fibroblast growth factor-2/brain- derived neurotrophic factor-associated maturation of new neurons generated from adult human subependymal cells. Ann. Neurol. 43, 576 – 585.

Plane JM, Liu R, Wang TW, Silverstein FS, Parent JM (2004) Neonatal hypoxic-ischemic injury increases forebrain subventricular zone neurogenesis in the mouse. Neurobiol Dis 16:585–595.

Raballo R, Rhee J, Lyn-Cook R, Leckman JF, Schwartz ML, Vaccarino FM (2000) Basic fibroblast growth factor (Fgf2) is necessary for cell proliferation and neurogenesis in the developing cerebral cortex. J Neurosci 20:5012–5023.

Saigal S, Doyle LW (2008) An overview of mortality and sequelae of preterm birth from infancy to adulthood. Lancet 371:261–269.

Shibata, T., Yamada, K., Watanabe, M., Ikenaka, K., Wada, K., Tanaka, K., Inoue, Y., 1997. Glutamate transporter GLAST is expressed in the radial glia-astrocyte lineage of developing mouse spinal cord. J. Neurosci. 17, 9212–9219.

Shin DM, Korada S, Raballo R, Shashikant CS, Simeone A, Taylor JR, Vac- carinoF (2004) Loss of glutamatergic pyramidal neurons in frontal and temporal cortex resulting from attenuation of Fgfr1 signaling is associated with spontaneous hyperactivity in mice. J Neurosci 24:2247–2258.

Skranes, J., Vangberg, T.R., Kulseng, S., Indredavik, M.S., Evensen, K.A., Martinussen, M., Dale, A.M., Haraldseth, O., Brubakk, A.M., 2007. Clinical findings and white matter abnormalities seen on diffusion tensor imaging in adolescents with very low birth weight. Brain 130, 654–666.

Smith KM, Ohkubo Y, Maragnoli ME, Rasin MR, Schwartz ML, Sestan N, Vaccarino FM (2006) Midline radial glia translocation and corpus callosum formation require FGF signaling. Nat Neurosci 9:787–797.

Srinivasan, L., Dutta, R., Counsell, S.J., Allsop, J.M., Boardman, J.P., Rutherford, M.A., Edwards, A.D., 2007. Quantification of deep gray matter in preterm infants at term-equivalent age using manual volumetry of 3-tesla magnetic resonance images. Pediatrics 119, 759–765.

Stavridis MP, Lunn JS, Collins BJ, Storey KG (2007) A discrete period of FGF-induced Erk1/2 signaling is required for vertebrate neural specification. Development 134:2889 – 2894.

Tao Y, Black IB, DiCicco-Bloom E (1996) Neurogenesis in neonatal rat brain is regulated by peripheral injection of basic fibroblast growth factor (bFGF). J Comp Neurol 376:653– 663.

Thompson, P.M., Cannon, T.D., Narr, K.L., van Erp, T., Poutanen, V.P., Huttunen, M., Lonnqvist, J., Standertskjold-Nordenstam, C.G., Kaprio, J., Khaledy, M., Dail, R., Zoumalan, C.I., Toga, A.W., 2001. Genetic influences on brain structure. Nat. Neurosci. 4, 1253–1258.

Trokovic R, Trokovic N, Hernesniemi S, Pirvola U, Vogt Weisenhorn DM, Rossant J, McMahon AP, Wurst W, Partanen J (2003) Fgfr1 is independently required in both developing mid- and hindbrain for sustained response to isthmic signals. EMBO J 22:1811–1823.

Turner CP, Seli M, Ment L, Stewart W, Yan H, Johansson B, Fredholm BB, Blackburn M, Rivkees SA (2003) A1 adenosine receptors mediate hypoxia-induced ventriculomegaly. Proc Natl Acad Sci U S A 100:11718 –11722.

Vaccarino FM, Schwartz ML, Raballo R, Rhee J, Lyn-Cook R (1999a) Fibroblast growth factor signaling regulates growth and morphogenesis at multiple steps during brain development. In: Current topics in developmental biology (Pedersen RA, Shatten G, eds), pp 179–200. San Diego: Academic.

Vaccarino FM, Schwartz ML, Raballo R, Nilsen J, Rhee J, Zhou M, Doetschman T, Coffin JD, Wyland JJ, Hung YT (1999b) Changes in cerebral cortex size are governed by fibroblast growth factor during embryogenesis. Nat Neurosci 2:246 –253.

Vaccarino FM, Ganat Y, Zhang Y, Zheng W (2001) Stem cells in neurodevelopment and plasticity. Neuropsychopharmacology 25:805– 815.

Wagner JP, Black IB, DiCicco-Bloom E (1999) Stimulation of neonatal and adult brain neurogenesis by subcutaneous injection of basic fibroblast growth factor. J Neurosci 19:6006 – 6016.

Weiss J, Takizawa B, McGee A, Stewart WB, Zhang H, Ment L, Schwartz M, Strittmatter S (2004) Neonatal hypoxia suppresses oligodendrocyte Nogo-A and increases axonal sprouting in a rodent model for human prematurity. Exp Neurol 189:141–149.

Yang, Z., Levison, S.W., 2006. Hypoxia/ischemia expands the regenerative capacity of progenitors in the perinatal subventricular zone. Neuroscience 139, 555–564.

Yang Z, Covey MV, Bitel CL, Ni L, Jonakait GM, Levison SW (2007) Sus- tained neocortical neurogenesis after neonatal hypoxic/ischemic injury. Ann Neurol 61:199 – 208.

Yoshimura S, Takagi Y, Harada J, Teramoto T, Thomas SS, Waeber C, Bakowska JC, Breakefield XO, Moskowitz MA (2001) Fgf2 regulation of neurogenesis in adult hippocampus after brain injury. Proc Natl Acad Sci U S A 98:5874 –5879.

Zhao T, Zhang CP, Liu ZH, Wu LY, Huang X, Wu HT, Xiong L, Wang X, Wang XM, Zhu LL, Fan M (2008) Hypoxia-driven proliferation of embryonic neural stem/progenitor cells–role of hypoxia-inducible transcription factor-1alpha. FEBS J 275:1824 –1834.

Zheng W, Nowakowski RS, Vaccarino FM (2004) Fibroblast growth factor 2 is required for maintaining the neural stem cell pool in the mouse brain subventricular zone. Dev Neurosci 26:181–196.

Zhuo L, Theis M, Alvarez-Maya I, Brenner M, Willecke K, Messing A (2001) hGFAP-cre transgenic mice for manipulation of glial and neuronal function in vivo. Genesis 31:85–94.